doi:10.1093/brain/awq360 Brain 2011: 134; 464–483 | 464

BRAIN
A JOURNAL OF NEUROLOGY

In vivo monitoring of neuronal loss in traumatic brain injury: a microdialysis study

Axel Petzold,[1,2,3] Martin M. Tisdall,[2] Armand R. Girbes,[3] Lillian Martinian,[4] Maria Thom,[4] Neil Kitchen[5] and Martin Smith[6]

1 Department of Neuroimmunology, UCL Institute of Neurology, Queen Square, London, WC1N 3BG, UK
2 The Tavistock Intensive Care Unit and Department of Neurosurgery, The National Hospital for Neurology and Neurosurgery, London, WC1N 3BG, UK
3 Department of Intensive Care, VU Medical Centre, Amsterdam 1081 HV, The Netherlands
4 Division of Neuropathology, UCL Institute of Neurology, Queen Square, London, WC1N 3BG, UK
5 Department of Neurosurgery, The National Hospital for Neurology and Neurosurgery, London, WC1N 3BG, UK
6 Centre for Neuroanaesthesia and The Tavistock Intensive Care Unit, The National Hospital for Neurology and Neurosurgery, London, WC1N 3BG, UK

Correspondence to: Axel Petzold,
Department of Neuroimmunology,
The National Hospital for Neurology and Neurosurgery,
Queen Square,
London, WC1N 3BG, UK
E-mail: a.petzold@ion.ucl.ac.uk

Traumatic brain injury causes diffuse axonal injury and loss of cortical neurons. These features are well recognized histologically, but their *in vivo* monitoring remains challenging. *In vivo* cortical microdialysis samples the extracellular fluid adjacent to neurons and axons. Here, we describe a novel neuronal proteolytic pathway and demonstrate the exclusive neuro-axonal expression of Pavlov's enterokinase. Enterokinase is membrane bound and cleaves the neurofilament heavy chain at positions 476 and 986. Using a 100 kDa microdialysis cut-off membrane the two proteolytic breakdown products, extracellular fluid neurofilament heavy chains $NfH_{476-986}$ and $NfH_{476-1026}$, can be quantified with a relative recovery of 20%. In a prospective clinical *in vivo* study, we included 10 patients with traumatic brain injury with a median Glasgow Coma Score of 9, providing 640 cortical extracellular fluid samples for longitudinal data analysis. Following high-velocity impact traumatic brain injury, microdialysate extracellular fluid neurofilament heavy chain levels were significantly higher (6.18 $\pm$ 2.94 ng/ml) and detectable for longer ($>$4 days) compared with traumatic brain injury secondary to falls (0.84 $\pm$ 1.77 ng/ml, $<$2 days). During the initial 16 h following traumatic brain injury, strong correlations were found between extracellular fluid neurofilament heavy chain levels and physiological parameters (systemic blood pressure, anaerobic cerebral metabolism, excessive brain tissue oxygenation, elevated brain temperature). Finally, extracellular fluid neurofilament heavy chain levels were of prognostic value, predicting mortality with an odds ratio of 7.68 (confidence interval 2.15–27.46, $P = 0.001$). In conclusion, this study describes the discovery of Pavlov's enterokinase in the human brain, a novel neuronal proteolytic pathway that gives rise to specific protein biomarkers ($NfH_{476-986}$ and $Nf_{H476-1026}$) applicable to *in vivo* monitoring of diffuse axonal injury and neuronal loss in traumatic brain injury.

Keywords: extracellular fluid; interstitial fluid; neurocritical care; neurodegeneration; neurofilaments

Abbreviations: GCS = Glasgow Coma Score; GOS = Glasgow Outcome Score; NfH = neurofilament heavy chain; NfL = neurofilament light chain; NfM = neurofilament medium chain

Received April 28, 2010. Revised September 21, 2010. Accepted October 22, 2010

Introduction

Traumatic brain injury is a major cause of death and one of the most frequent neurological disorders. An estimated 1.4 million US individuals suffer from traumatic brain injury per year (Langlois *et al*., 2006*a*). Mortality is higher with road traffic accidents (27–34%) compared with falls (10–11%) (Adekoya and Majumder, 2004). Following road traffic accidents, fire-arm injury and assault are the other two main causes for severe traumatic brain injury (Langlois *et al*., 2006*b*; Minino *et al*., 2006). High-velocity impact injuries of any type are of particular concern (Kirkpatrick, 1983; Suneson *et al*., 1990; Gieron *et al*., 1998; Corbo and Tripathi, 2004; Bakir *et al*., 2005; Walilko *et al*., 2005). Neurological morbidity results predominantly from cognitive and behavioural problems causing a reduced quality of life due to loss of independence and productivity (Dikmen *et al*., 1995). Neuroaxonal degeneration is a likely cause for morbidity and mortality after traumatic brain injury, but is difficult to monitor in the living human subject (Povlishock, 1992; Smith, 2003).

In their seminal paper, Gennarelli *et al*. (1982) show that rotational accelerations are the main contributor to diffuse axonal injury in a primate model. Additionally, driver-dummy data from vehicle impact testing suggest that rotational accelerations contribute to over 80% of the brain strain independent of crash mode (Zhang *et al*., 2006). These data are in line with neuropathological studies in humans showing substantial loss of neurons in the subcortical grey matter following traumatic brain injury (Graham *et al*., 1992, 2005). Consistent with the post-mortem observations is experimental work showing that traumatic brain injury causes diffuse, widespread neuronal damage in addition to focal brain injury. Hall *et al*. (2005) demonstrated in a mouse model that neurodegeneration affected all layers of the ipsilateral cortex, starting within 6 h after impact. Diffuse degeneration affected neurons in the hippocampus and thalamus (layer CA1, CA3) and their connections (efferent CA1 pyramidal axons, mossy fibres, Schaffer collaterals and the perforant path), as well as the corpus callosum and visual cortex (Hall *et al*., 2005). The onset of cytoskeletal degradation after experimental traumatic impact was found to be as fast as 30 min (Deng *et al*., 2007). The final common pathway results in cellular calcium overload that activates the enzyme calpain, causing intracellular proteolysis (Deng *et al*., 2007; McGinn *et al*., 2009). Following this enzymatically mediated degradation, the cytoskeletal proteins and their breakdown products are released into the extracellular fluid. Among these is a group of proteins known as neurofilaments, which are highly specific for the neuroaxonal compartment (Shaw, 1998; Buki and Povlishock, 2006; Petzold, 2007). In the CNS, neurofilaments are made up of four subunits, a light (68 kDa), medium (150 kDa) and heavy (190–210 kDa) chain alongside α-internexin (Shaw, 1998; Petzold, 2005).

In this study, we show for the first time that a specific biomarker for neuronal–axonal degeneration (Shaw, 1998; Petzold, 2007) can be quantified *in vivo* from the human cortical extracellular fluid (Vespa *et al*., 2005; Tisdall and Smith, 2006). In a proof of principle study, we tested whether levels of this protein biomarker are related to (i) the *in vitro* neuronal count; (ii) *in vitro* characteristics of the microdialysis system; (iii) the phenotype *in vivo* (Gennarelli *et al*., 1982; Kirkpatrick, 1983; Suneson *et al*., 1990; Gieron *et al*., 1998; Corbo and Tripathi, 2004; Bakir *et al*., 2005; Walilko *et al*., 2005; Zhang *et al*., 2006); (iv) brain imaging (Marshall *et al*., 1992; Steyerberg *et al*., 2008); (v) other *in vivo* markers associated with neuroaxonal degeneration (Buki and Povlishock, 2006) and (vi) prognosis in traumatic brain injury.

Materials and methods

Patients

Patients suffering from a traumatic brain injury who were admitted to the Neurosurgical Intensive Care Unit at the National Hospital for Neurology and Neurosurgery were recruited between January 2006 and February 2007. Inclusion criteria were (i) traumatic brain injury; (ii) age $\geqslant$16 years; (iii) requirement for intra-cranial pressure monitoring in accordance with published guidelines [(PMID: 10937893) 2000] and (iv) that written, informed, witnessed consent could be obtained from the next of kin. Exclusion criteria included (i) polytrauma; (ii) significant thoracic or abdominal injuries; (iii) documented pre-admission hypotensive (systolic blood pressure $<$90 mmHg) or (iv) hypoxic (peripheral oximetry saturation $<$90%) episodes. High-velocity impact traumatic brain injury was defined based on mechanism of injury (road traffic accidents, fire-arm, and assault) (Kirkpatrick, 1983; Adekoya and Majumder, 2004; Walilko *et al*., 2005; Langlois *et al*., 2006*b*; Minino *et al*., 2006). Severity of injury was additionally classified clinically based on the admission Glasgow Coma Score (GCS) into mild (GCS 13–15), moderate (GCS 9–12) and severe (GCS $\leqslant$8).

Brain imaging

All patients underwent computerized tomography (CT). The CT brain imaging was classified according to the Marshall criteria (Marshall *et al*., 1992; Steyerberg *et al*., 2008), the presence of traumatic subarachnoid blood (Steyerberg *et al*., 2008) or an extradural haematoma (Steyerberg *et al*., 2008).

Procedures and sample collection

The microdialysis catheter (100 kDa molecular weight cut-off, CMA71, 20 mm length, 0.6 mm diameter polyamide membrane) was implanted through a triple lumen intra-cranial bolt (Technicam Ltd, Newton, Abbott, UK) in pericontusional tissue (in cases of contusion injury) or into the right frontal cortex (in cases of diffuse axonal injury) in agreement with consensus guidelines (Bellander *et al*., 2004). The catheter was perfused with commercially available artificial CSF (NaCl 147 mM, KCl 2.7 mM, CaCl 1.2 mM, MgCl 0.85 mM as supplied by CMA). The catheter was perfused at a constant flow rate of 0.3 μl/min. The system was allowed to equilibrate for 1 h prior to starting sample collection as per consensus guidelines (Bellander *et al*., 2004). Samples were collected on an hourly basis and frozen within 10 min of collection. The position of the gold labelled probes was verified on subsequent CT scans (except in Patient 5 were the catheter was inserted very late and Patient 9 were the catheter was removed very early). Intra-cranial pressure (Codman microsensor, Randolph, Ma, USA), brain temperature and calibrated brain tissue

oxygenation were recorded continuously (1 min intervals) using the LICOX device (Integra LifeSciences Corporation). Hourly mean values for these variables were calculated and confirmed by one physician (M.T.).

Cortical brain tissue samples

Post-mortem cortical tissue from traumatic brain injury cases ($n = 4$) were taken from areas close to macroscopically visible contusions. Control cortical post-mortem tissue was taken from two patients who died of a non-neurological condition. In addition, control brain tissue samples were collected from patients undergoing surgery for intractable epilepsy ($n = 3$). Tissue samples were fixed with formalin prior to embedding in paraffin.

Patient management

Patients were sedated with propofol and fentanyl and received protocol-guided stepwise therapy based on the Brain Trauma Foundation guidance (Kitson, 2005) to maintain a cerebral perfusion pressure above 60 mmHg. As part of the intra-cranial pressure management, patients were mechanically ventilated to maintain a CO_2 partial pressure of 4.0–4.5 kPa. Blood glucose was maintained between 4.0 and 9.0 mM using an insulin (i.v. actrapid) sliding scale. Management of the patients was not affected by involvement in the study.

Outcome measure

Two clinical endpoints were collected: (i) survival on discharge from hospital and (ii) the Glasgow Outcome Score (GOS) at 3 months and 6 months after injury. The GOS was dichotomized into unfavourable recovery (GOS: 1 indicates death; 2, persistent vegetative state and 3, severe disability) or favourable recovery (GOS: 4 indicates moderate disability; 5, good recovery) (Teasdale *et al.*, 1998).

Sample analysis

In each patient, the microdialysis probe was allowed to stabilize for 1 h (Bellander *et al.*, 2004). Only samples collected after this equilibration period were investigated. At the end of each 1 h collection period, the microdialysate of the extracellular fluid was immediately analysed for lactate and pyruvate with the bedside CMA 600 Analyser (CMA Microdialysis) using an enzymatic colourimetric technique (Afinowi *et al.*, 2009). For quality control analysis, artificial CSF samples were analysed on a calibrated YSI 2003 STAT Plus Glucose and Lactate Analyser (YSI Inc., Yellow Springs, Ohio, USA) and compared with the values derived by the CMA 600 Analyser. The batch-frozen samples were pooled in 3 h intervals and extracellular fluid neurofilament heavy chain (NfH) levels were measured using an in-house developed and externally validated enzyme-linked immunosorbent assay (Petzold *et al.*, 2003; Petzold and Shaw, 2007). All samples were analysed in duplicates and repeated if the coefficient of variation was greater than the intra-assay precision of 10% (Petzold *et al.*, 2003). The analyst was blinded to all other information.

Recovery

Recovery experiments were carried out as previously described (Afinowi *et al.*, 2009). Large volume (100 ml) CSF samples ($n = 12$) were used as source solutions. Microdialysis pumps (CMA 106; CMA Microdialysis AB, Solna, Sweden) were used at a constant flow rate of 0.3 μl/min. The *in vitro* relative recovery was calculated as:

$$\text{Relative recovery (\%)} = \text{dialysate concentration} : \text{reference solution concentration} \times 100.$$

Gel electrophoresis

Following the NfH enzyme-linked immunosorbent assay, surplus of the extracellular fluid samples was kept at 4°C. Extracellular fluid samples with high NfH content were pooled. Due to the small remaining sample size after performing the enzyme-linked immunosorbent assay, a total of 84 microvials from five patients were pooled to give 250 μl of extracellular fluid, known to have a high NfH concentration. The pooled extracellular fluid was mixed with 170 μl lithium dodecyl sulphate, 10 μl dithiothreitol and heated at 65°C to unfold the proteins. The sample (400 μl) was loaded onto the 4–12% Bis–Tris and 3–8% Tris–acetate gels. Molecular weight markers (Invitrogen, MagicMark, Western Standard and SeeBlue Plus2, Invitrogen) were used for each run. The gels were run under reducing conditions (Invitrogen System, PowerEase 500, 200 V, 120 mA, 25 W).

Immunoblot

The proteins were transferred from the gel to a nitrocellulose membrane over a 2 h blotting period (25 V, 160 mA, 17 W). The membrane was blocked in 2% fat milk powder/0.9% saline for 1 h. Blocking solution was decanted and the membrane was washed five times for 3 min with washing solution (0.1% fat milk powder/0.9% saline, 0.1% Tween-20). The membranes were either incubated with the first antibody in a single well or adjusted between two plastic layers and sealed in a manifold (Hoefer) so that each of the 10 channels overlaid the entire area onto which the proteins have been transferred. The channels were each filled with 3 ml of 0.1% fat milk powder/0.9% saline, containing antibodies different antibodies in a 1:1000 dilution. For detection of NfH, six mouse monoclonal antibodies directed at different phosphoepitopes (see Table 1 in Petzold *et al.*, 2003) were used: SMI 32, SMI 34, SMI 35, SMI 37, SMI 38 and SMI 311 (originally purchased from Sternberger Monoclonals Incorporated, now Covance Research Products, Berkeley CA, USA). In addition, antibodies to the neurofilament light chain (NfL) and medium chain (NfM) were also used (NR4 mouse monoclonal anti-NfL from Sigma and rabbit polyclonal anti-NfM from Affinity, UK). Antibodies were incubated at 4°C overnight on a shaker. After decanting the antibodies, each channel was washed five times for 3 min with washing solution. The channels were then filled with the appropriate horseradish peroxidase-labelled detector antibody (swine anti-rabbit or rabbit anti-mouse, both Sigma) and incubated for 1 h at room temperature. Antibodies were decanted and the membranes were washed in each channel for 5 min, 10 times. The membranes were incubated with the chemiluminescence substrate (SuperSingal West Pico, Thermo Scientific, #34078) for 5 min. The dried membranes were visualized on an AlphaEase FluorChem SP CCD camera.

Dephosphorylation and proteolysis

HPLC-purified bovine NfH was diluted into glycine buffer (pH 10.4) at a concentration of 50 μg/ml. NfH was dephosphorylated with 100 mU of alkaline phosphatase (ALP, EC 3.1.3.1, Sigma, P4252) at 37°C for 1 h (Petzold *et al.*, 2008). Aliquots of phosphorylated NfH and dephosphorylated NfH were incubated with (i) enterokinase (EC 3.4.21.9,

Table 1 Neuronal apoptosis in traumatic brain injury

ID	Age (gender)	Tissue	Brain area	Condition	Caspase-3
Patient 1	85 (F)	Post-mortem	Contusion, SDH, ICH	Traumatic brain injury	+
Patient 2	73 (F)	Post-mortem	Contusion	Traumatic brain injury	+
Patient 3	83 (M)	Post-mortem	Contusion	Traumatic brain injury	+
Patient 4	51 (M)	Post-mortem	Contusion	Traumatic brain injury	+
Patient 5	39 (F)	Post-mortem	Temporal lobe	Normal control	–
Patient 6	35 (F)	Post-mortem	Temporal lobe	Normal control	±
Patient 7	48 (M)	Surgery	Temporal lobe	Epilepsy	–
Patient 8	34 (M)	Surgery	Temporal lobe	Epilepsy	–
Patient 9	47 (F)	Surgery	Temporal lobe	Epilepsy	–

Neuronal staining for caspase-3: – = absent, ± = uncertain, + = positive. ICH = intra-cranial haemorrhage; SDH = subdural haematoma.

Roche, Cat No 11 334 115 001) and (ii) α-chymotrypsin (CT, EC 3.4.21.1, Sigma, C-4129).

Laser capture microdissection

PC6-3 cells, a derivate from the PC12 cell line, were converted into neuronal-like cells as described by Pittman *et al.* (1993). The cells were grown in Roswell Park Memorial Institute medium, 10% horse serum, 5% foetal calf serum and penicillin/streptomycin. For differentiation, the cells were switched to Roswell Park Memorial Institute medium, 2% horse serum, 1% foetal calf serum + 100 ng/ml nerve growth factor. The cells were then mounted on polyethylene naphthalate membrane-covered glass slides. The cells were washed three times with phosphate buffered saline and fixed in 70% ethanol. The cells were air dried and the Laser Microbeam System (P.A.L.M., Microlaser Technologies AG, Munich, Germany) was used under visual control to capture the cells in barbitone buffer (pH 8.9) used for enzyme-linked immunosorbent assay (Schutze *et al.*, 2007).

Protein extraction from snap frozen brain tissue

Protein extraction was modified from the method previously described (Ericsson *et al.*, 2007). Lithium dodecyl sulphate was added to the samples at 50 times the dry weight of the frozen brain tissue samples. All samples were sonicated on ice in a polypropylene tube. Samples were then incubated at 70°C for 10 min. After rigorous mixing at 1400 rpm samples were centrifuged at $13.2 \times 10g$ for 10 min at 4°C. The supernatant was used for western and immunoblotting.

Immunohistochemistry

Sections (7 μm) were dewaxed and rehydrated followed by 15 min incubation in 3% hydrogen peroxide and deionized water followed by microwave heat treatment. Protein blocking was carried out with normal horse serum. Sections were incubated overnight at room temperature with anti-goat enterokinase antibody (1:300 Santa Cruz Biotechnology, Inc., CA 95060, USA) using Vector ImmPRESS™ anti goat detection system kit (Vector Labs: Burlington, CA, USA) and visualized with diaminobenzidine chromogen. Sections were washed with phosphate buffered saline + 0.05% Tween-20 in each step. Control sections were treated the same but the primary antibody was omitted. Neuronal apoptosis was assessed by staining for caspase-3 (1:500, Clone 269518, Code MAB 835, R&D System, Minneapolis, USA) as described (Sulejczak *et al.*, 2008; Sairanen *et al.*, 2009; Umschwief *et al.*, 2010).

Immunofluorescence

The same procedure was used as that for immunohistochemistry up until the incubation of the antibodies. Sections were incubated with enterokinase antibody first at 1:400 dilution followed by secondary ImPRESS anti-goat then Fluorescein Green Tyramide Signal Amplification (PerkinElmer Life and Analytical Sciences, Boston, MA, USA). After washing, the sections were quenched with 1% hydrogen peroxide for 15 min in order to prevent any deposited tyramide combining with the second tyramide signal that followed. After washing, protein blocking was done with normal horse serum (Vector laboratories) followed by incubation with primary monoclonal antibody SMI32 (1:500, Covance, Emeryville, CA, USA) and monoclonal neurofilament 200 (NE14, 1:3000, Sigma, St Louis, Missouri 63103, USA). Sections were incubated with relevant secondary horseradish peroxidase detection system followed by CY3 from the Tyramide Signal Amplification Kit. Sections were mounted on Vectashield® with Dapi (Vector laboratories) and visualized with a Leica confocal laser microscope. After each step sections were washed with phosphate buffered saline. Negative controls were treated the same except the primary antibodies were omitted.

Data analysis

Statistical analyses were performed using SAS software (V9.2). Independent variables were compared using the non-parametric two-sample exact Wilcoxon rank-sum test for two variables and a two-way unbalanced ANOVA (general linear model) for more than two variables. Repeated measurement analysis was performed on 3 h epochs (pooled extracellular fluid sampling time) using mixed models. The best fitting model was selected based on the best fitting covariance structure (Littell *et al.*, 1998). The linear relationship between continuous variables was evaluated using the Spearman correlation coefficient. The level of significance for the multiple correlations was corrected using the Bonferroni method. The Chi-Square-test and Fisher's exact test were used for comparing proportion of patients. Two-tailed tests were used throughout and P-values of <0.05 were accepted as significant.

Results

Neurofilaments are a protein biomarker for neuronal loss

As a proof of principle, an *in vitro* cell culture set-up was used to investigate the relationship between the NfH protein concentration and the number of PC12 cells (Fig. 1A). Individual PC12 cells were collected using laser-capture microdissection (Schutze *et al.*, 2007). A minimum of 50 PC12 cells were needed for detection of NfH in the enzyme-linked immunosorbent assay (Petzold *et al.*, 2003). The linear relationship ($R = 0.98$, $P = 0.013$) of laser-captured PC12 cells with NfH levels equated to: PC12 cells number = 1245 × NfH − 46 (Fig. 1B). In PC12 cells, NfH accounted only to 0.011% of the total soluble cellular protein fraction which was 24.6 times <0.271% quantified from human grey matter ($P = 0.0014$, Fig. 1C).

The relative recovery of NfH from a solute is influenced by the pore size of the microdialysis membrane (Fig. 1E). The *in vitro* recovery experiment showed a significant loss of NfH from the source solute compared with samples recovered either through a 20 or 100 kDa microdialysis membrane [general linear model, $F(2, 33) = 171$, $P < 0.0001$, Fig. 1F]. The mean relative recovery of NfH for the 100 kDa membrane (CMA71, 20 mm length, 0.6 mm diameter polyamide membrane) was 20.7 ± 3.2 (Fig. 1G). For the 20 kDa membrane (CMA70, 20 mm length, 0.6 mm diameter polyamide membrane) the relative recovery

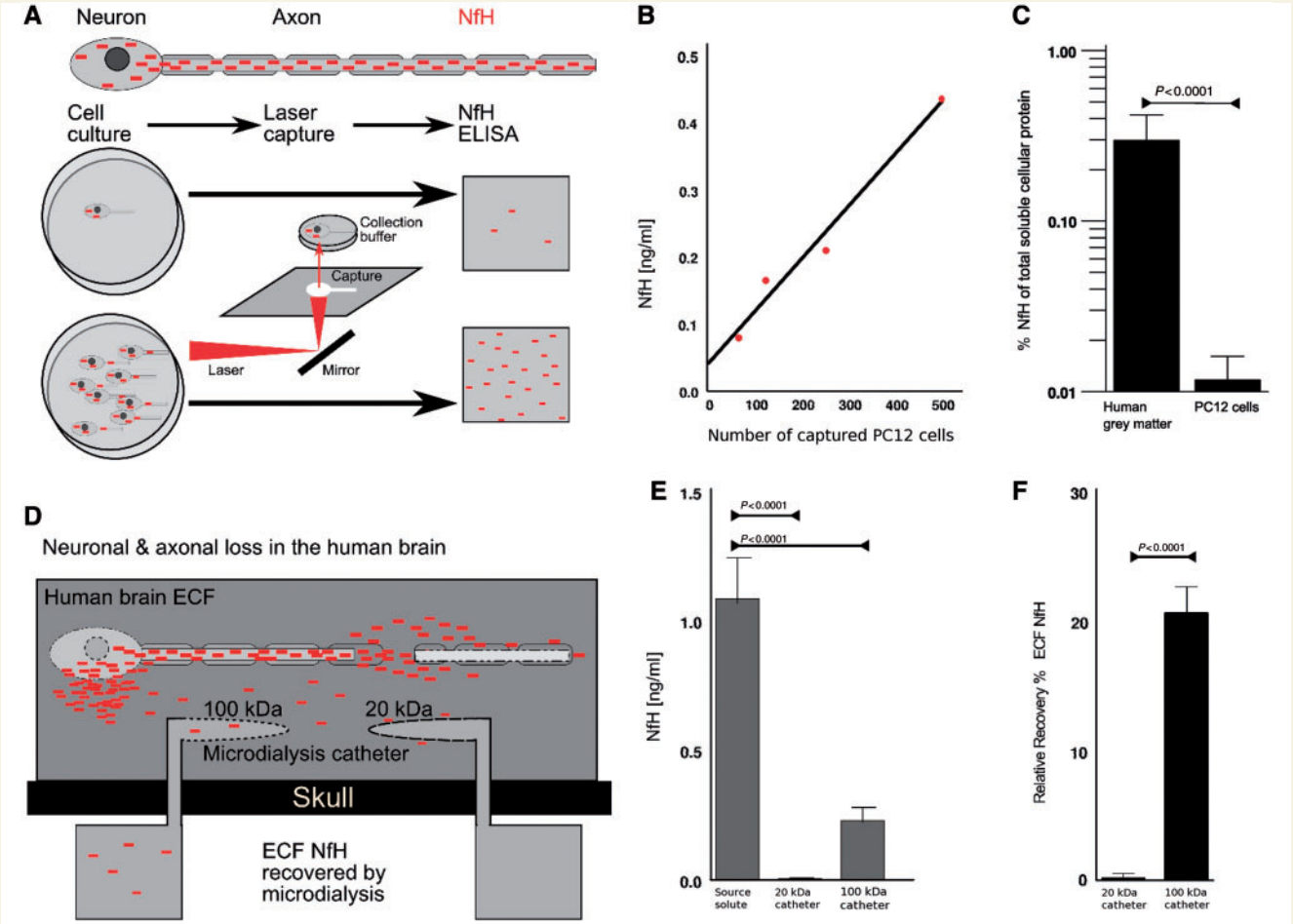

Figure 1 Neurofilaments are a protein biomarker for neuronal loss. (**A**) The cytoskeleton of the neuron and axon contains the neurofilament heavy chain (NfH, filled red boxes). The number of laser-captured neurons/axons relates to the NfH levels quantified by enzyme-linked immunosorbent assay. (**B**) The estimated quantitative relationship between the number of laser-captured PC12 cells and the NfH concentration is expressed as: (number of PC12 cells ~1245 × NfH − 46, $R = 0.98$, $P = 0.013$). The lowest number of laser-captured cells giving for quantifiable NfH levels was 50 (data not shown). (**C**) The percentage of NfH to total soluble protein is 24.6 times higher in the human grey matter compared with PC12 cells. (**D**) In the injured human brain, NfH is released from the neuronal compartment into the extracellular fluid (ECF, dark grey box). Placement of a microdialysis catheter into the human cortex, adjacent to neurons, allows recovery of NfH from the human extracellular fluid. (**E**) The *in vitro* recovery experiment showed that NfH could be recovered from a source solute using a 100 kDa microdialysis catheter, but not a 20 kDa catheter. (**F**) Consequently, the relative recovery of NfH was negligible for the 20 kDa catheter and 20% for the 100 kDa microdialysis catheter.

was negligible at $0.2 \pm 0.4\%$ (Kruskal–Wallis, $\chi^2 = 18.23$, $P < 0.0001$).

Neurofilament heavy chain cleavage products are recovered from human extracellular fluid

Pooled human extracellular fluid with high and low NfH levels were used to investigate how this large protein (1020 amino acids corresponding to a molecular mass of 113 kDa) could be recovered through a 100 kDa catheter membrane. Of note, most of the literature refers to the molecular mass derived from sodium dodecyl sulphate gels which is in the 190–210 kDa range. The difference between these molecular weight values is explained by altered electrophoretic mobility caused by the charge/weight of the bound phosphate (Petzold, 2005). Using gel electrophoresis we demonstrated that high molecular weight proteins were present in extracellular fluid with high NfH levels but not in extracellular fluid with low NfH levels (Fig. 2A). The immunoblot showed immunoreactivity of a protein with SMI34 (Fig. 2B). The immunoreactivity appears to be specific for the NfH phosphoforms SMI32, SMI38, SMI34, SMI35, SMI37 and SMI311, as there was no cross-reactivity with antibodies against NfM and NfL (Fig. 2C). Comparative immunoblotting shows identifies two NfH cleavage products in the 100–120 kDa range (Fig. 2D, Lane 2 and Fig. 2E, Lanes 2 and 7).

The described *in vivo* cleavage products can be reproduced *in vitro* by incubation of purified NfH with enterokinase (Fig. 2D, Lane 4 and Fig. 2E, Lane 8). The electrophoretic mobility of the extracellular fluid NfH cleavage products ($NfH_{476-986}$ and $NfH_{476-1026}$) matches what can be expected from the known NfH enterokinase cleavage sites (Fig. 2F). The corresponding molecular weight of $NfH_{476-986}$ and $NfH_{476-1026}$ calculated from the amino acid sequence of the cleavage product corresponds to 56–60 kDa (Fig. 2F). In this article, the extracellular fluid NfH cleavage products will be referred to as extracellular fluid NfH.

A novel neuronal proteolytic pathway

The immunohistochemistry shows the presence of enterokinase in the frontal cortex of a patient with traumatic brain injury (Fig. 3A). Mainly large neurons and their axons are stained. There was almost no immunoreactivity to enterokinase in the deep white matter (data not shown). Enterokinase was not found in endothelial cells, astrocytes or microglia. The exclusively neuronal expression of enterokinase is not specific for traumatic brain injury because a similar staining pattern is also seen in patients with epilepsy (Fig. 3B). The immunohistochemistry suggests that the heavy subunit of enterokinase may be membrane bound. This observation is confirmed by the immunofluorescence (Fig. 3C and D). The predominant expression of the enterokinase heavy chain in the human cortex, but not deep white matter, is confirmed by immunoblotting (Fig. 3E). In a subpopulation of large neurons, enterokinase colocalizes with phosphorylated NfH (Fig. 3C).

Apoptosis of cortical neurons in traumatic brain injury

In all traumatic brain injury post-mortem cases there are apoptotic caspase-3 positive cells in the vicinity of the contusion (Table 1). Staining for caspase-3 was essentially absent from normal control post-mortem tissue and temporal lobar tissue removed during epilepsy surgery (Table 1). The morphological analysis of the caspase-3 cells identifies different types of neurons including pyramidal cells (Fig. 4A and B). Many of the caspase-3 positive cells were degenerate and apoptotic.

Patients

The clinical characteristics of the 10 patients with traumatic brain injury recruited into this prospective, longitudinal study are summarized in Table 2. Nine patients were male and one was female. The median age was 39 years (range 20–68 years). The severity of the injury ranged from mild to severe with a median admission GCS of 9 (range 4–15). The individual CT brain scans documenting the brain pathology and the position of the microdialysis catheter are shown in Fig. 5.

Extracellular fluid neurofilament heavy chain in traumatic brain injury

A total of 640 microdialysis samples were collected on an hourly basis for this study. The median time between injury and catheter insertion was 14 h (range 7–37 h) when considering all but one patient (Patient 5) who was referred to us with a 5 day delay.

The individual extracellular fluid NfH levels are shown in Fig. 5. An early peak of the extracellular fluid NfH concentration was observed in 7/10 (70%) of patients (Patients 1, 3, 4, 6, 7, 8 and 9; indicated by single arrows in Fig. 5). In addition, secondary peaks of extracellular fluid NfH were observed in eight patients (Patients 1, 2, 3, 4, 5, 6, 7 and 10; indicated by double arrows in Fig. 5). In four patients the concentration of extracellular fluid NfH measured in secondary peaks during the later disease course exceeded what was observed initially (Patients 2, 3, 7 and 10). Due to small sample volume in Patient 5, it was only possible to measure extracellular fluid NfH 25 h after catheter insertion. Patient 5 showed an early peak of extracellular fluid NfH at ~0.4 ng/ml. The longitudinal data on extracellular fluid lactate and extracellular fluid pyruvate values in this patient, directly following catheter insertion, suggest that this extracellular fluid NfH peak was not likely to be a consequence of a catheter insertion artefact (Supplementary Fig. 1).

Phenotypic analyses

We classified road traffic accidents in three patients and assault in one patient (Patient 5) as high-velocity impact traumatic brain injury. However, the actual impact of injury was not recorded (see below). A fall was the cause of traumatic brain injury in the remaining six patients (Table 2). Patients who suffered from high-velocity impact traumatic brain injury had considerably higher early extracellular fluid NfH levels compared with those

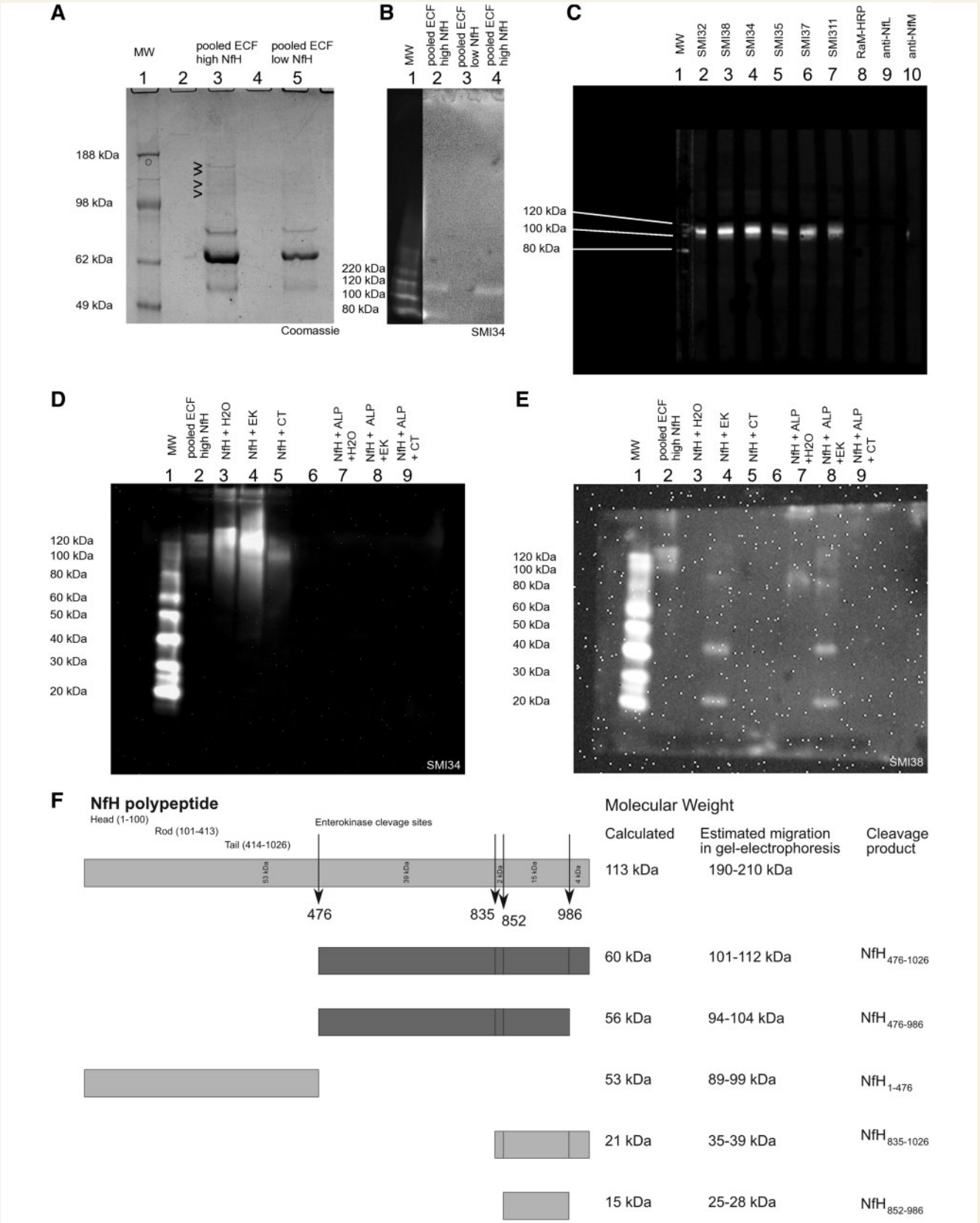

Figure 2 Identification of five new NfH enterokinase cleavage products. (**A**) Gel electrophoresis of pooled extracellular fluid (ECF) (4–12% Bis-Tris gel, Coomassie stain). There are a number of distinct bands visible between 98 and 188 kDa in extracellular fluid pooled (100 kDa catheter) from samples with high NfH, which can not be visualized from the extracellular fluid of samples with non-measurable NfH. (**B**) The immunoblot shows a ~100 kDa protein recognized by SMI34 in the extracellular fluid pooled from samples with a high NfH

(continued)

suffering from a fall. The averaged extracellular fluid NfH levels over the initial 24 h were 7-fold higher (6.18 ± 2.94 ng/ml) following high-velocity impact traumatic brain injury compared with a fall (0.84 ± 1.77 ng/ml). Moreover, extracellular fluid NfH levels remained for longer on a high level following high-velocity impact traumatic brain injury [$F(19, 344) = 28.72$, $P < 0.0001$, Fig. 6A]. Following a fall, the extracellular fluid NfH levels declined steadily to become non-detectable after an average of 2 days.

In patients with a high-velocity impact traumatic brain injury, the extracellular fluid lactate to pyruvate ratio was above 25 at onset and the longitudinal profile was different compared with the lactate to pyruvate ratio in traumatic brain injury after fall [$F(18, 366) = 3.67$, $P < 0.0001$, Fig. 6B]. Similarly, there was a mild but significant difference in the brain temperature profile [$F(18, 297) = 5.89$, $P < 0.0001$, Fig. 6D]. Finally, the intra-cranial pressure remained higher in patients with traumatic brain injury with a fall compared with high-velocity impact traumatic brain injury throughout the entire observation period [$F(18, 370) = 1.94$, $P = 0.012$, Fig. 6G]. None of the other physiological parameters distinguished between the two groups (Fig. 6C, E, F and H).

Because the impact of injury was not recorded, additional analyses were performed comparing three categories: road traffic accidents, assault and falls. There was a significant overall difference between these three groups over time for extracellular fluid NfH levels ($F = 3.41$, $P = 0.0049$) and brain temperature ($F = 8.13$, $P < 0.0001$). However, significance was lost for the extracellular fluid lactate to pyruvate ratio ($F = 0.35$, $P = 0.91$) and intra-cranial pressure ($F = 0.50$, $P = 0.81$).

Injury severity was classified according to the GCS into mild ($n = 3$), moderate ($n = 2$) and severe ($n = 5$) traumatic brain injury. There was no significant difference for extracellular fluid NfH levels according to the GCS [$F(5, 481) = 0.14$, $P = 0.98$].

Brain imaging analyses

There was a significant difference in extracellular fluid NfH levels over time in patients with traumatic brain injury with traumatic subarachnoid blood ($n = 3$) compared with those without traumatic subarachnoid blood [$n = 7$, $F(19, 343) = 4.07$, $P < 0.0001$].

No such differences were found for patients with traumatic brain injury with extradural haematoma compared with those without (data not shown). Likewise, there were no significant differences for extracellular fluid NfH levels according to the Marshall CT brain imaging classification (Marshall *et al*., 1992) (data not shown).

Physiological correlations

A correlation analysis was performed using the multimodal monitoring data set focusing on four physiological parameters that have been related to injury severity and outcome in traumatic brain injury (Enblad *et al*., 2001; Hutchinson *et al*., 2002; Butcher *et al*., 2007; Arieli *et al*., 2008; Belli *et al*., 2008; Diringer, 2008; Polderman, 2008; Stiver and Manley, 2008). Figure 7A shows the statistical strength of the correlation (Spearman's R) between these parameters and extracellular fluid NfH levels.

Lactate to pyruvate ratio

There was a strong and significant correlation between the lactate to pyruvate ratio and extracellular fluid NfH levels in the initial three epochs ($R = 0.83$ to $R = 0.63$, Fig. 7A). The raw data for the second epoch show that extracellular fluid NfH levels started to rise with a lactate to pyruvate ratio >20 (Fig. 7B).

Figure 2 Continued
concentration (Lanes 2 and 4) but not from samples with non-measurable NfH levels (Lane 3). No other higher molecular weight NfH fragments were recovered through the 100 kDa microdialysis membrane (3–8% Tris–acetate gel, because of overexposure of the molecular weight markers (MW), the gain for Lane 1 was digitally reduced). (**C**) The ~100 kDa protein fragment is recognized by monoclonal antibodies against phosphorylated (SMI34, SMI35) and non-phosphorylated (SMI32, SMI38, SMI37, SMI311) NfH epitopes. The strongest immunoreactivity was observed with SMI34 and SMI38. There was no binding to the detecting rabbit anti-mouse horseradish peroxidase labelled antibody (RaM-HRP). Equally, there was no binding with monoclonal antibodies against NfL or NfM, known to have a small degree of cross-reactivity with the NfH head/rod region. This suggests that the recovered protein stems from the NfH tail region (4–12% Bis-Tris, 1 well gel, antibody incubation in manifold). (**D**) Immunoreactivity against hyperphosphorylated NfH (SMI34). The 100–120 kDa band from human extracellular fluid (Lane 2) migrates in a similar range to a fraction present in HPLC-purified bovine NfH (Lane 3), which can be further enhanced by limited proteolysis with enterokinase (EK, Lane 4) but not α-chymotrypsin (CT, Lane 4). Not all of the purified higher molecular weight NfH migrates into the gel (top part of Lanes 3–4). There is no immunoreactivity of SMI34 with dephosphorylated purified or proteolysed NfH (Lanes 7–9). (**E**) Immunoreactivity against non-phosphorylated NfH (SMI38). The 100–120 kDa band from human extracellular fluid (Lane 2) migrates in the same range as partially enterokinase proteolysed non-phosphorylated NfH (Lane 8). Enterokinase proteolysis reveals three additional bands (~90, 40, 20 kDa) for both phosphorylated (Lane 4) and non-phosphorylated NfH (Lane 8). (**F**) Cleavage of NfH with enterokinase occurs at four sites (ExPASy, peptide cutter), leaving 12 hypothetical proteolytic fragments, five of which probably explain the immunoreactivity against SMI38 (Lanes 4 and 8 in **E**). Cleavage at position 476 alone (first dark grey box) or positions 476 and 986 (second dark grey box) is thought to produce the polypeptides giving rise to the immunoreactivity against SMI34 and SMI38 seen in the 100–120 kDa range (Lanes 1 and 3 in **D**, Lanes 1 and 8 in **E**). The immunoreactivity of the phosphorylated NfH 35–39 kDa and 25–28 kDa fragments (bottom two light grey boxes) with the non-phosphoepitope specific monoclonal antibody SMI38 (Lane 4 in **E**) may be explained by structure related dephosphorylation of a serine residue (e.g. at position 865), adjacent to the enterokinase cleavage sites or alternatively by limited phosphatase activity of enterokinase. ALP = alkaline phosphatase.

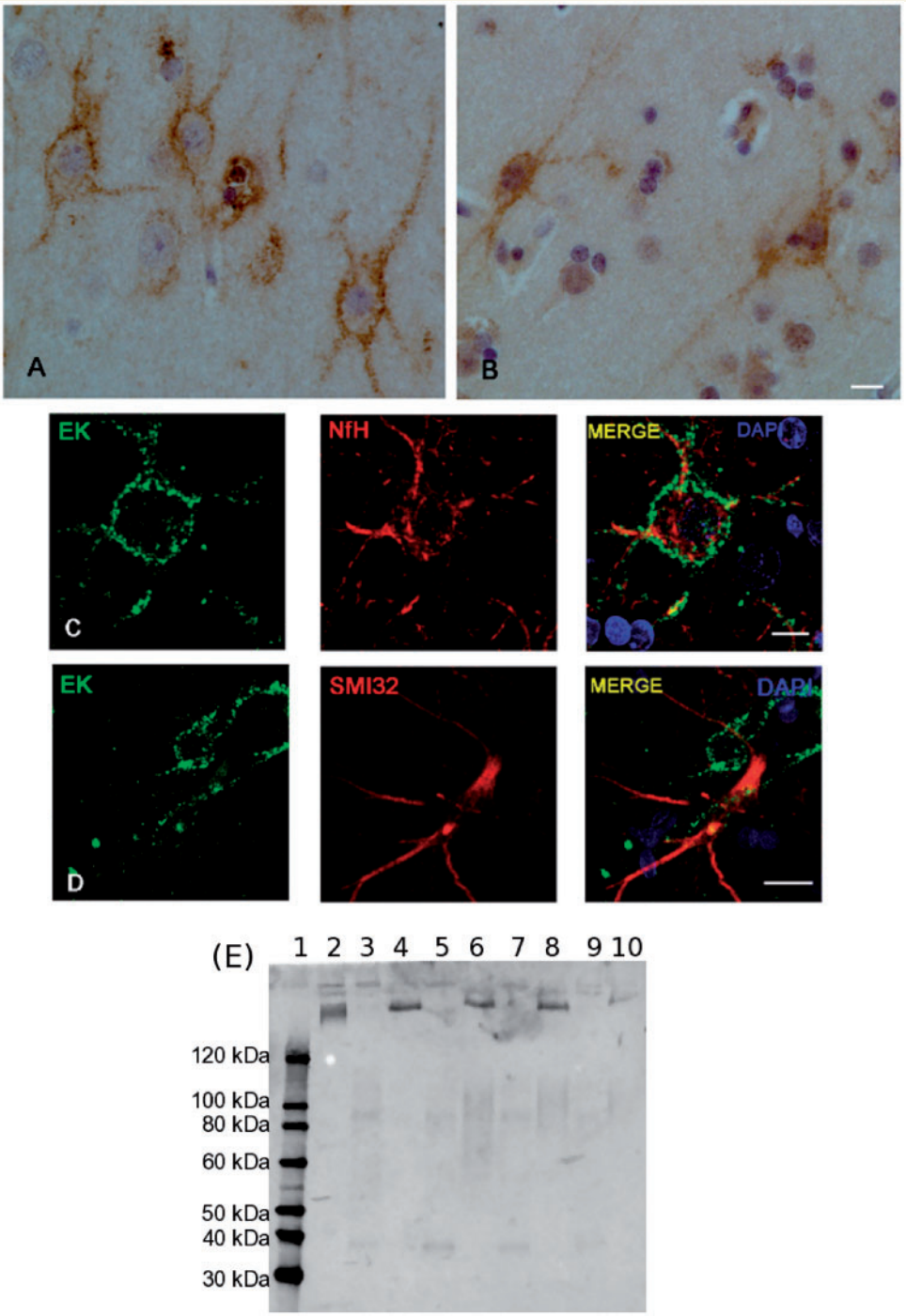

Figure 3 Enterokinase is expressed in cortical neurons and axons. (**A**) Immunohistochemistry demonstrates that cortical neurons and their axons are selectively stained for enterokinase (frontal lobe, traumatic brain injury). Enterokinase appears to localize to the membrane of neurons and axons (scale bar = 10 μm). (**B**) A similar staining pattern for enterokinase is seen in control tissue (frontal lobe, epilepsy). This suggests that enterokinase is expressed in a subset of human cortical neurons and not a specific phenomenon seen in traumatic brain injury (scale bar = 10μm). (**C**) Confocal imaging shows that large neurons positive for enterokinase also stain for phosphorylated NfH in traumatic brain injury (scale bar = 10 μm). (**D**) Enterokinase was not found in neurons, which predominantly expressed dephosphorylated NfH SMI32 in traumatic brain injury (scale bar = 25 μm). (**E**) The immunoblot shows presence of the heavy chain of enterokinase in homogenated human cortex (four traumatic brain injury cases, Lanes 4, 6, 8 and 10), but not in adjacent white matter tissue (Lanes 3, 5, 7 and 9). There is a mild degree of cross-reactivity of the antibody (LC13) with the enterokinase light chain, seen for the purified protein only (Lane 2, ~50 kDa). The molecular weight markers are shown in Lane 1.

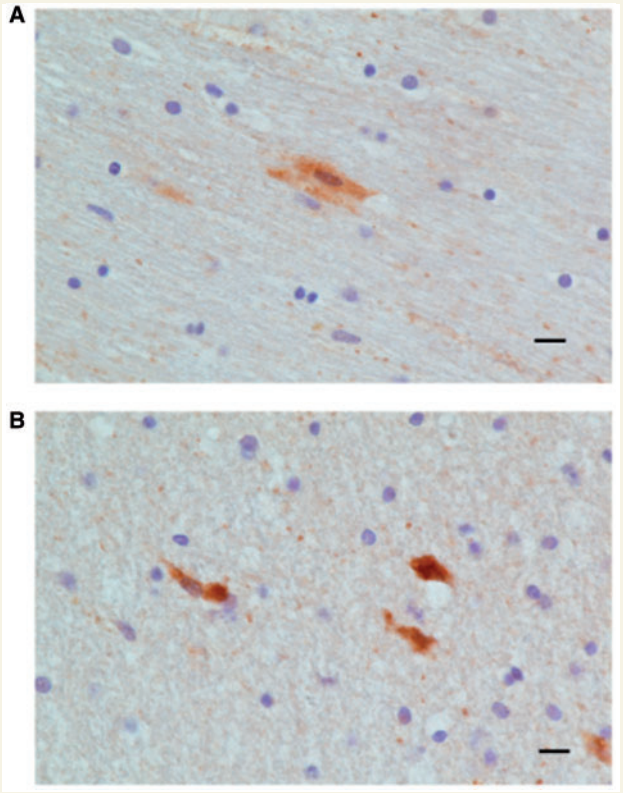

Figure 4 Apoptosis of cortical neurons in traumatic brain injury. (**A**) Caspase-3 positive pyramidal cells in the vicinity of a cortical contusion from a patient with traumatic brain injury (cases 18–95). (**B**) Caspase-3 positive neuronal like cells with dendritic processes in the vicinity of the contusion area of another patient with traumatic brain injury. Scale bar = 10 μm.

Systemic blood pressure

The mean arterial blood pressure correlated significantly with extracellular fluid NfH levels between the second and fifth epoch ($R = -0.75$ to $R = -0.46$, Fig. 7A) and during the later course when cerebral perfusion pressure management became critical (Fig. 6H). During the epoch where the correlation of the mean arterial blood pressure with extracellular fluid NfH levels was the strongest (Epoch 4, $R = -0.75$, $P < 0.0001$), there was also an inverse correlation of the cerebral perfusion pressure with extracellular fluid NfH levels ($R = -0.67$, $P = 0.0001$, Fig. 7A). The raw data show the highest extracellular fluid NfH levels for a mean arterial blood pressure below 90 mmHg (Fig. 7D).

Brain oxygenation

There was a moderate correlation of the brain tissue oxygenation with extracellular fluid NfH levels ($R = 0.85$ to $R = 0.73$, Fig. 7A). The raw data for the second epoch show that this correlation was due to a scatter of high CSF NfH levels for brain tissue oxygenation levels above 30 kPa (Fig. 7F).

Brain temperature

There was a significant correlation between higher brain temperature and extracellular fluid NfH levels ($R = 0.72$ to $R = 0.51$, Fig. 7A). The raw data show the highest extracellular fluid NfH levels for a brain temperature above 37°C (Fig. 7H).

Prognosis

The last hypothesis tested was that extracellular fluid NfH levels may be of prognostic value in traumatic brain injury (Buki and Povlishock, 2006; Petzold, 2007). Five (50%) of the 10 patients

Table 2 Patients demographics

ID	Age (gender)	High impact traumatic brain injury	Admission Eyes Verbal Motor (GCS)	CT brain imaging	Other injury	Comorbidity	Catheter position	Time to death (days)	GOS (3 months)	GOS (6 months)
1	57 (F)	+	E4V4M6 (14)	R temporal fracture, tSAH, EDH, SDH	Clavicular fracture	Hypothyroidism	R frontal	5	1	1
2	45 (M)	–	E1V1M1 (5)	L SDH, tSAH	None	None	L frontal	6	1	1
3	48 (M)	–	E4V5M6 (15)	frontal fracture, contusions	None	None	L frontal	4	1	1
4	32 (M)	+	— (11)	R SDH	None	None	R frontal	—	4	4
5	22 (M)	+	E2V2M6 (10)	L parietotemporal fracture, SDH	None	None	R frontal	—	4	4
6	68 (M)	–	— (14)	R SDH, R ICH, R contusions	None	None	R frontal	—	2	2
7	44 (M)	–	E1V1M5 (7)	tSAH, contusions	None	None	L frontal	5	1	1
8	27 (M)	–	E2V2M4 (8)	L EDH, tSAH	None	None	R frontal	5	1	1
9	20 (M)	+	E1V1M5 (7)	R temporal fracture, EDH	None	None	R frontal	—	5	5
10	34 (M)	–	— (4)	L temporal fracture, L SDH, contusions, pontine ICH	None	None	L frontal	—	3	3

— = data not available; E = eyes; EDH = extradural haematoma; (F) = female; ICH = intra-cranial haemorrhage; L = left; (M) = male; M = motor; R = right; SDH = subdural haematoma; tSAH = traumatic subarachnoid haemorrhage, V = verbal.

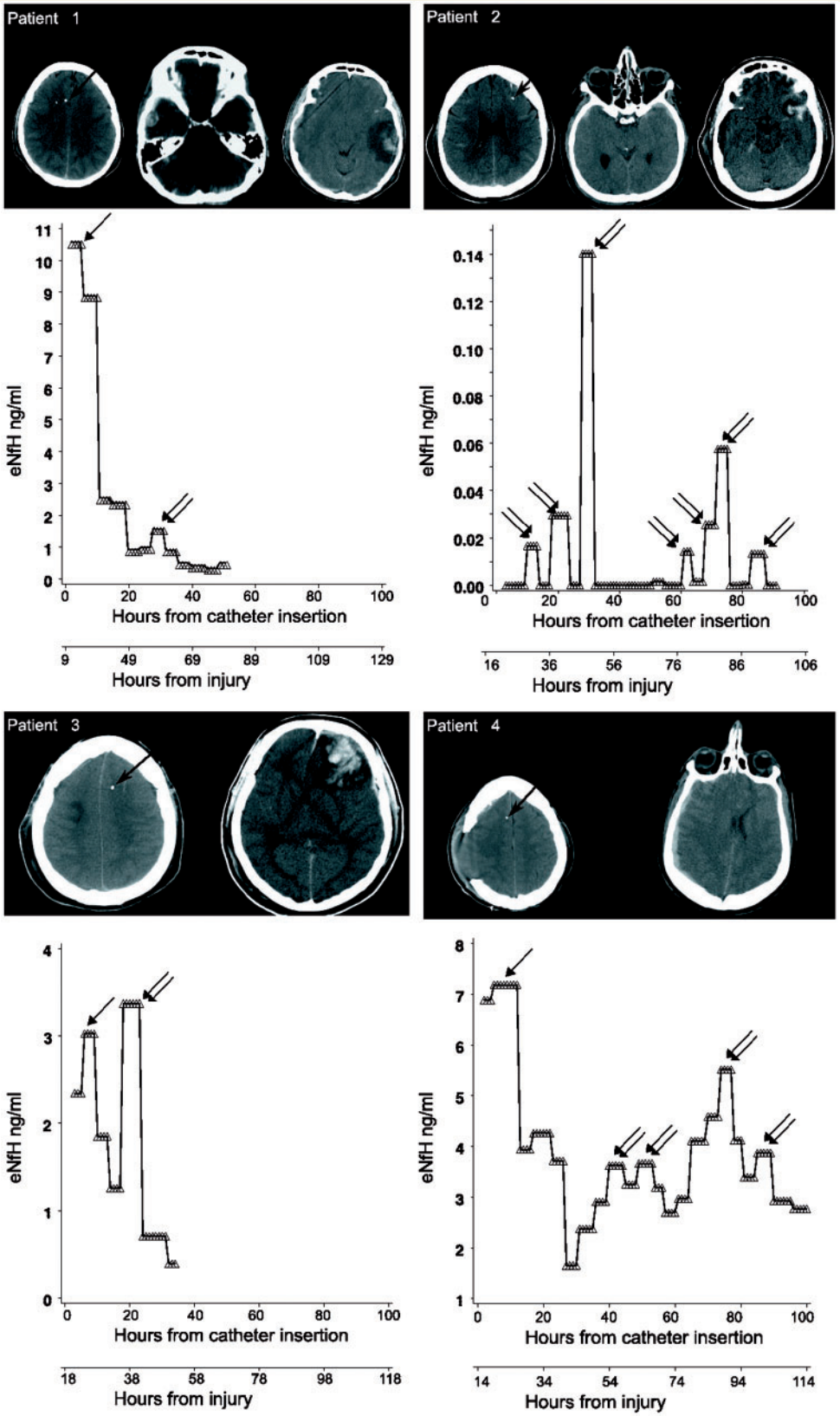

Figure 5 Extracellular fluid NfH levels in traumatic brain injury. The longitudinal profile of extracellular fluid NfH levels in individual patients is shown in relation to catheter localization, time from catheter insertion and time from injury. The tip of the catheter is indicated by a black arrow overlaid to the patients' CT brain scan. Early extracellular fluid NfH peaks are identified by single arrows. Secondary extracellular fluid NfH peaks occurring after a period of decreasing or consistently low extracellular fluid NfH levels are indicated by double arrows. Note that the scale for the *y*-axis is individually optimized for best visualization of extracellular fluid NfH levels.

(continued)

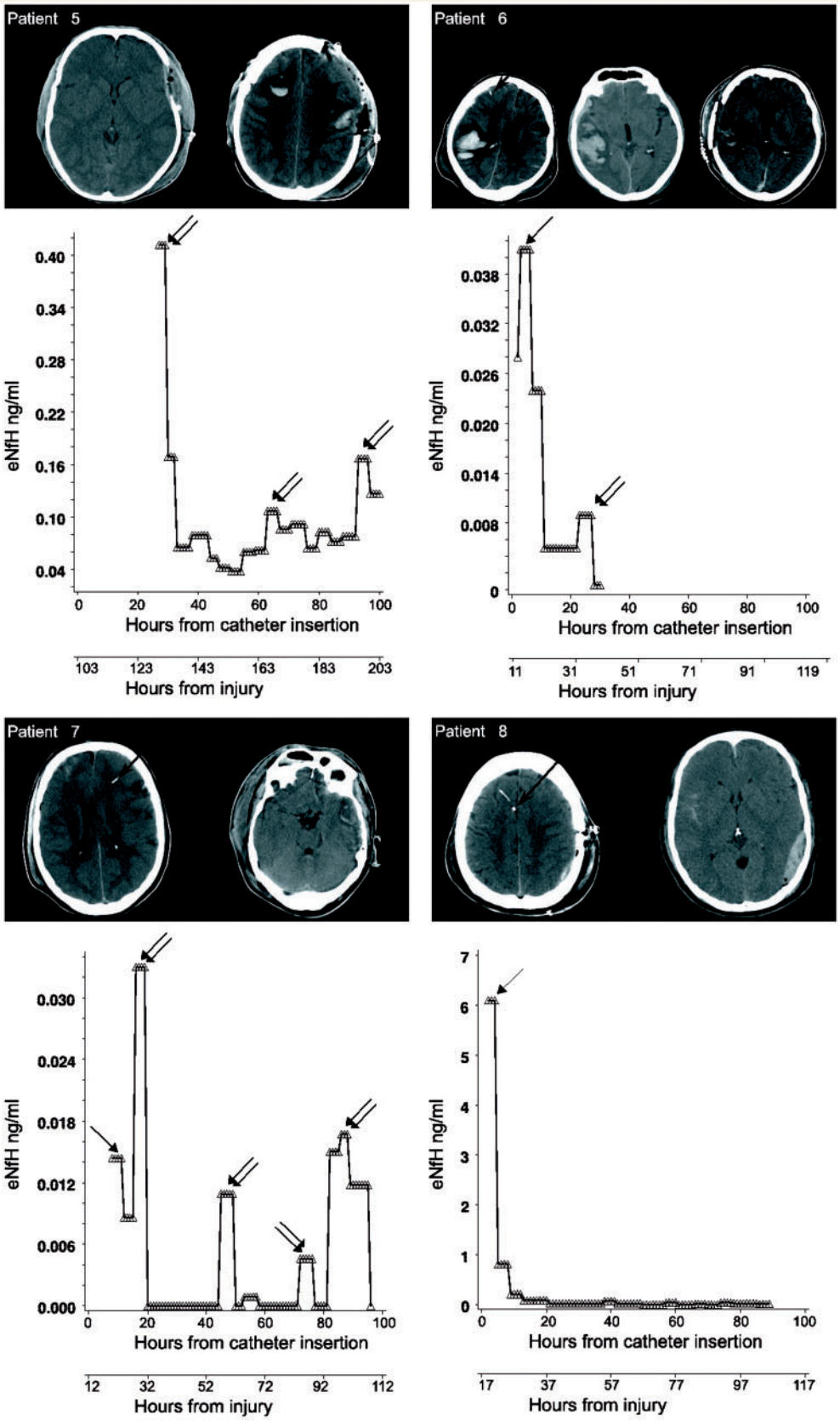

Figure 5 Continued.

(continued)

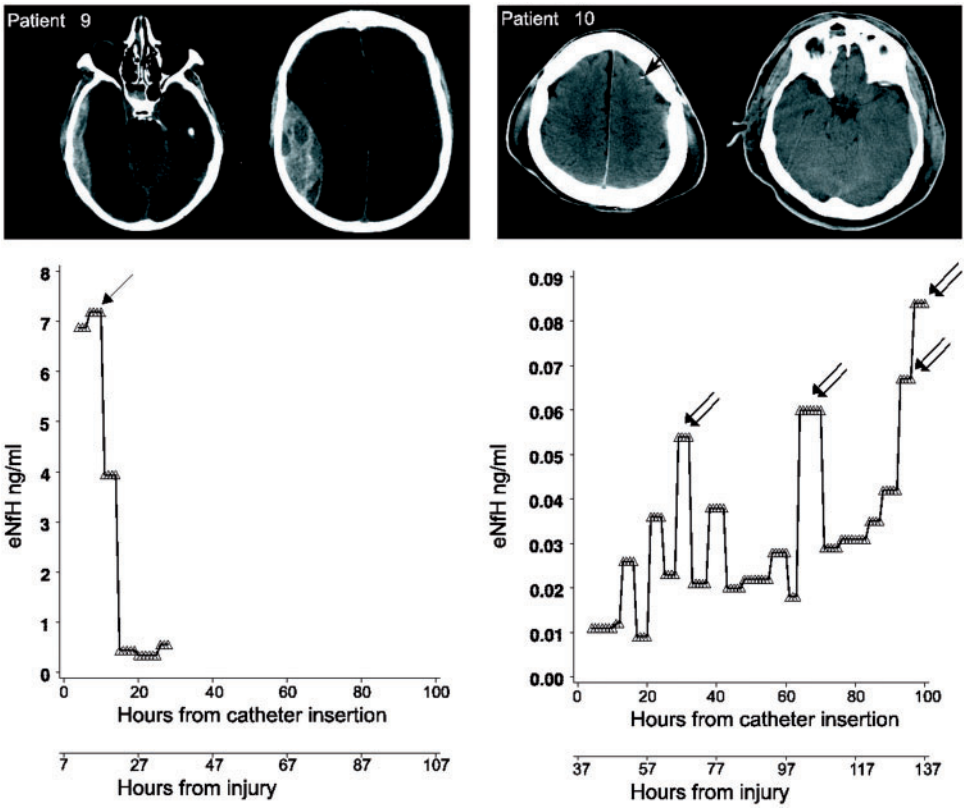

Figure 5 Continued.

with traumatic brain injury died within a median of 5 days (range 4–6 days) following the injury (Table 2).

The individual percentage of hours with pathological values for the sampled physiological parameters spanning the entire observation period (up to 230 h post-traumatic brain injury) are shown in Table 3. These physiological parameters were more frequently pathological in non-survivors compared with survivors for intra-cranial pressure ($P < 0.0001$), lactate to pyruvate ratio >25 ($P = 0.0003$) or lactate to pyruvate ratio >40 ($P < 0.0001$), brain tissue oxygenation ($P < 0.0001$) and brain temperature ($P < 0.0001$), but not for the cerebral perfusion pressure ($P = 0.84$). Non-survivors had significantly more periods where the mean hourly lactate to pyruvate ratio was above our cut-off of 25 or Vespa's more conservative cut-off of 40 (Vespa *et al*., 2005; Belli *et al*., 2008) (Table 3).

The initial prognostic value of these physiological parameters and of extracellular fluid NfH levels were investigated with logistic regression models using survival as the outcome variable. Models were tested for validity based on the minimum observation period needed to reveal any meaningful prognostic information. Table 4 shows that after a 12 h observation period, the best predictor for mortality was extracellular fluid NfH levels with an odds ratio of 7.68 [95% confidence interval (95% CI) 2.15–27.46]. The other two strong predictors of mortality were the intra-cranial pressure (5.06, 95% CI 1.84–13.89) and admission GCS (4.13, 95% CI 1.72–9.94).

Discussion

In this translational, proof of principle study, we describe a specific biomarker (extracellular fluid NfH) related to a novel neuronal proteolytic pathway involving Pavlov's enterokinase (Ivan P. Pavlov, Russian neurologist, 1849–1936). Quantification of the enterokinase cleavage products neurofilament heavy chain ($NfH_{476-986}$ and $NfH_{476-1026}$) from the human extracellular fluid allowed for *in vivo* monitoring of neuronal loss in traumatic brain injury. The two discovered protein fragments are different to the 53 kDa and 57 kDa breakdown products with NfL immunoreactivity shown to appear ~3 h following traumatic brain injury *in vivo* and *in vitro* (Nixon and Sihag, 1991; Posmantur *et al*., 1998, 1994). The molecular weight of the observed NfH breakdown products is also less than the previously described 120 and 146 kDa fragments following calpain induced proteolysis (Greenwood *et al*., 1993), bearing in mind that these molecular weight data were based on electrophoretic mobility. This observation led to the discovery of enterokinase as the responsible proteolytic enzyme. The known consensus for enterokinase cleavage site, DDDDK (Boulware and Daugherty, 2006), is very similar to the cleavage sites found in NfH in our study, which are either EEEK or EEEEK. The presence of enterokinase in the human brain has not previously been reported. Enterokinase was originally discovered from the succus entericus of the dog (Schepowalnikow, 1899; Pavlov, 1910). Probably interested in intestinal movements

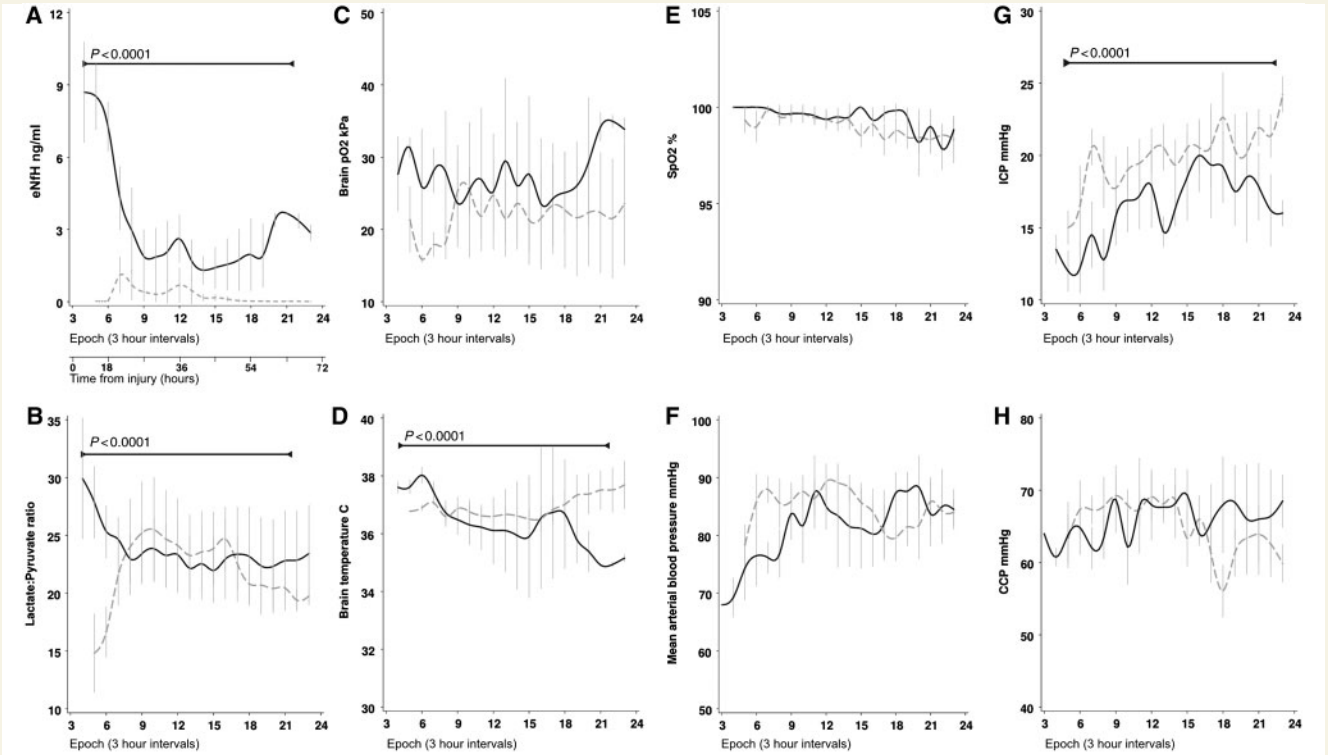

Figure 6 Multimodal monitoring illustrates that extracellular fluid NfH levels peaked in the acute phase of traumatic brain injury coinciding with derangement of physiological parameters. The mode of injury in patients with traumatic brain injury was either due to a fall (dotted line) or high-velocity impact traumatic brain injury (closed line). The multimodal data are plotted over time using 3 h epochs. (**A**) Extracellular fluid NfH levels were significantly higher in high impact traumatic brain injury compared with a fall ($P < 0.0001$). (**B**) The extracellular fluid lactate to pyruvate ratio was highest in high-velocity impact traumatic brain injury ($P < 0.0001$) suggesting critical energy demand under anaerobic metabolic conditions. (**C**) The brain tissue oxygenation (BtO_2) did not differ significantly between groups. (**D**) Initially the brain temperature (BT) was significantly higher in high-velocity impact traumatic brain injury ($P < 0.0001$), but a crossover of the curves occurred after six epochs, reflecting active cooling as part of intra-cranial pressure targeted management. (**E**) The systemic oxygen saturation (SpO_2) remained in the target range (>98%) throughout and did not differ significantly between the groups. (**F**) There were no periods of systemic hypotension. The mean arterial blood pressure (ABP) increased to >80 mmHg after nine epochs due to volume resuscitation and inotropic support as part of targeted intra-cranial pressure management. (**G**) The mean intra-cranial pressure (ICP) was significantly higher after a fall ($P < 0.0001$) and continued to increase. The critical threshold of 20 mmHg was passed after the 10th epoch. (**H**) Successful maintenance of the cerebral perfusion pressure (CPP) above 60 mmHg was achieved by increasing the mean arterial blood pressure until Epoch 15. From there on the continuous increase of intra-cranial pressure in patients with a fall started to affect the cerebral perfusion pressure. The means ± SD are shown.

associated with the Pavlov reflex (also called conditioned or acquired reflex), they named the enzyme enterokinase, a misnomer that is still widely used. In fact, the enzyme is a serine protease also known as enteropeptidase (Light and Janska, 1989). While our discovery is novel, it is perhaps not entirely surprising as the presence of other serine proteases that should depend on activation by enterokinase, such as trypsin, have been described in the brain (Wiegand *et al*., 1993; Blaber *et al*., 2002). Interestingly, co-compartmentalization of enterokinase with key modulators of the extracellular matrix (matrix metalloprotease-9, trypsin-2) has been reported in systemic carcinoma (Vilen *et al*., 2008). Future studies are needed to investigate whether enterokinase also plays a role in modulation of the extracellular matrix of the brain and thus in plasticity. The membrane bound colocalization of enterokinase with phosphorylated NfH may also indicate a role for neuronal reshaping during neuronal plasticity or for activation pathways of other brain proteases relevant to Alzheimer's disease (Leissring, 2008), immune-mediated demyelination (Blaber *et al*., 2002) and traumatic brain injury (Buki and Povlishock, 2006).

This serendipitous discovery aside, the results of our first two research hypotheses were instructive. In a proof of principle approach, we were able to show a linear relationship between number of laser-captured PC12 cells and NfH levels measured. A limitation of this approach, for methodological reasons, is that this cell line is known to express low levels of less phosphorylated NfH (Lindenbaum *et al*., 1987), which also—because of its different electrophoretic mobility—led to the suspicion that this NfH subunit may not be expressed by this cell line at all (Lee, 1985). Consistent with these data (Lee, 1985), others found phosphorylated NfH levels to be barely detectable from PC12 cells (Dashiell *et al*., 2002). In fact, the amount of NfH that we detected in PC12

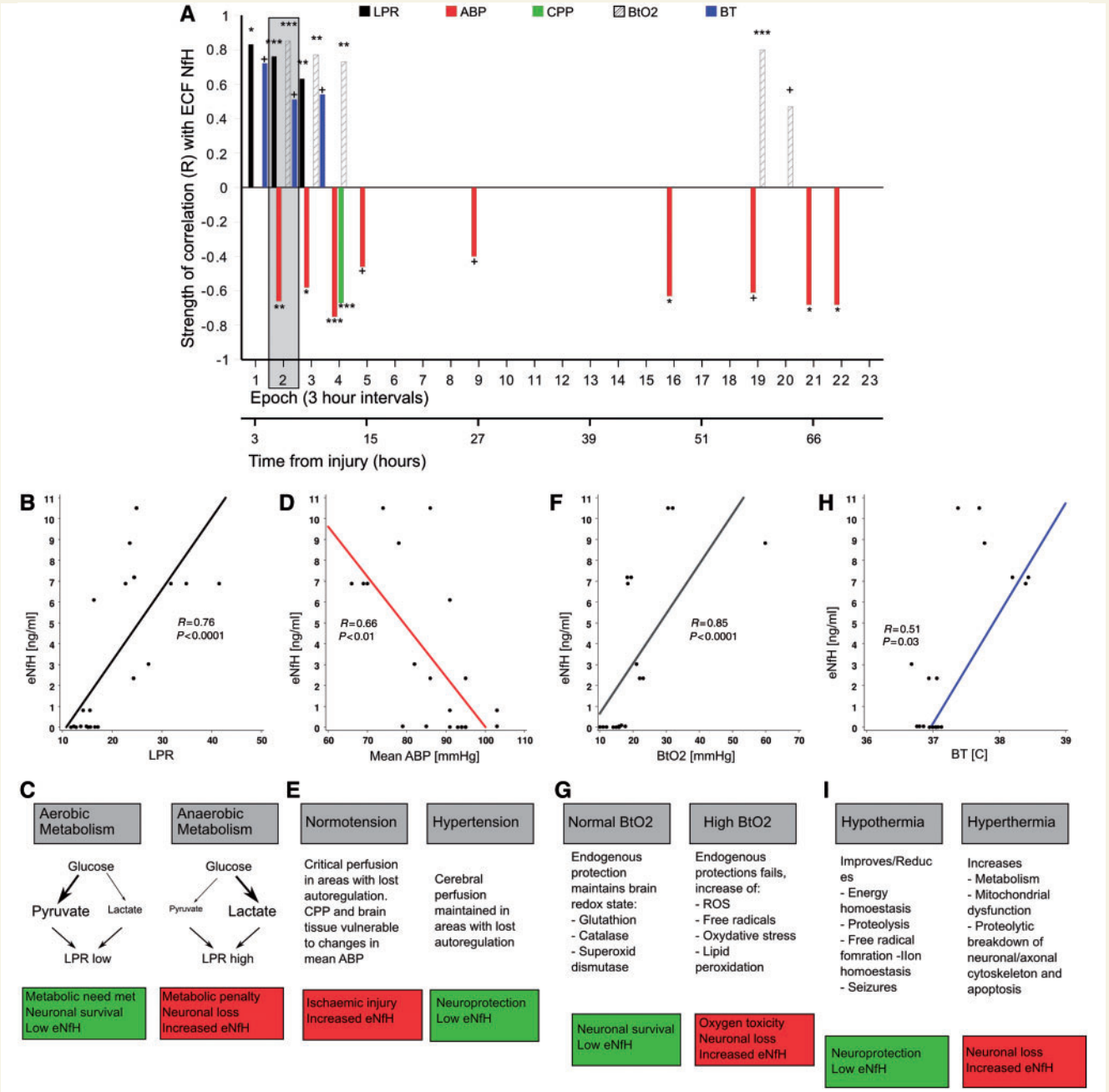

Figure 7 Mechanisms leading to neuronal loss and increase of extracellular fluid NfH. (**A**) The strength of significant correlations (Spearman's *R*, *y*-axis) between extracellular fluid NfH (eNfH) levels and physiological parameters during 3 h epochs (*x*-axis) is shown. The lactate to pyruvate ratio (LPR) is indicated by black bars, arterial blood pressure (ABP) by dark grey bars, cerebral perfusion pressure (CPP) by light green bars, brain tissue oxygenation (BtO_2) by hatched bars, brain temperature (BT) by blue bars. The grey box overlay highlights the correlations for which the raw data are shown. (**B**) The lactate to pyruvate ratio correlated with extracellular fluid NfH levels (Epoch 2). (**C**) Because the lactate to pyruvate ratio increases under anaerobic metabolic conditions, this suggests that the resulting metabolic penalty may cause neuronal loss with subsequent increase of extracellular fluid NfH. (**D**) The mean arterial blood pressure correlated inversely with extracellular fluid NfH levels. (**E**) This raises the question whether ischaemic neuronal injury may be reduced by more aggressive arterial blood pressure management. (**F**) The brain tissue oxygenation correlated with extracellular fluid NfH levels. (**G**) This suggests that increasing BtO_2 may saturate systems of endogenous protection. The resulting O_2 toxicity may cause neuronal injury resulting in increased levels of extracellular fluid NfH. (**H**) The brain temperature correlated with extracellular fluid NfH levels. (**I**) This suggests that higher brain temperature may accelerate mechanisms leading to neuronal apoptosis resulting in an increase of extracellular fluid NfH levels. ROS = reactive oxygen species, $^{***}P < 0.0001$, $^{**}P < 0.001$, $^{*}P < 0.01$, $^{\dagger}P < 0.05$.

Table 3 Physiological monitoring of hourly means

ID	Hours of recording	Time (%)					
		Intra-cranial pressure >20 (%)	Cerebral perfusion pressure <60 (%)	Lactate to pyruvate ratio >25 (%)	Lactate to pyruvate ratio >40 (%)	Brain tissue oxygenation <35 (%)	Brain temperature >38.1 (%)
1	89	17	8	79	0	65	0
2	102	62	17	5	1	99	0
3	50	70	46	91	0	92	0
4	353	20	15	12	1	73	27
5	174	0	4	53	25	93	87
6	48	8	19	71	3	93	0
7	31	16	3	42	0	97	44
8	110	46	18	0	0	4	30
9	32	6	41	93	7	NA	0
10	230	60	31	0	0	99	51

The percentage of hours with pathological values are shown. For the lactate to pyruvate ratio, two cut-off values are used i.e. 25 (published by Belli *et al*. 2008) and the higher cut-off of 40 (published by Vespa *et al*. 2005). NA = not available.

Table 4 Odds ratio for predicting mortality in traumatic brain injury

Marker	ORs	95% CI	*P*-value
Extracellular fluid NfH	7.68	2.15–27.46	0.001
Intra-cranial pressure	5.06	1.84–13.89	0.001
GCS	4.13	1.72–9.94	0.001
Cerebral perfusion pressure	1.55	1.14–2.12	<0.01

cells was only ~0.011% of the total soluble cell protein fraction, which is 5–8 times less than what others found for tau protein (~0.08% of total protein) or for microtubule associated protein 1 (~0.05% of total protein, after 3 days in culture, see Fig. 2 in Drubin *et al*., 1985). This limitation prevents the use of NfH data to estimate the absolute numbers of neurons lost in the human brain, as the human neurons contain ~24.6 times more NfH than PC12 cells.

Testing our second research hypothesis, we found a relative *in vitro* recovery of extracellular fluid NfH of ~20%. Thus the relative recovery was substantially less than that of smaller compounds such as pyruvate or lactate (Hutchinson *et al*., 2005; Afinowi *et al*., 2009), which may limit the quantification of extracellular fluid NfH to scenarios involving a substantial degree of neuronal and axonal loss. Substantial damage to the neurons and their adjacent axons loss is seen in traumatic brain injury (Gennarelli *et al*., 1982; Graham *et al*., 1992, 2005).

In line with the *in vitro* experiments, extracellular fluid NfH was detectable *in vivo* in patients with traumatic brain injury. It should be noted that, in four patients, the concentration of extracellular fluid NfH measured in secondary peaks during the later disease course exceeded that observed initially. This observation makes it unlikely that extracellular fluid NfH levels may be artefactually high due to possible catheter insertion related parenchymal damage (Bellander *et al*., 2004). Additionally, we strictly adhered to consensus guidelines recommending a 1 h catheter equilibration period prior to analysis (Bellander *et al*., 2004). In one patient (Patient 5), catheter insertion was delayed (5 days after impact), therefore this patient may allow for a better distinction between possible insertion artefact and traumatic brain injury-related injury. The lactate and pyruvate data collected after insertion are in the normal range and make an insertion artefact most unlikely (Supplementary Fig. 1). In an additional post-mortem study and consistent with the literature (Graham *et al*., 1992, 2005), we demonstrated neuronal apoptosis in the cortex of patients with traumatic brain injury. Neuronal apoptosis was identified using caspase-3 immunostaining (Sulejczak *et al*., 2008; Sairanen *et al*., 2009; Umschwief *et al*., 2010). There were essentially no caspase-3 positive neurons in controls using either post-mortem tissue or higher quality neurosurgical tissue from patients undergoing epilepsy surgery. Therefore, we interpret the initial extracellular fluid NfH peaks seen as evidence for primary neuronal injury and the secondary peaks of neuronal damage due to secondary brain damage. Taken together, the data provide *in vivo* evidence that the major loss of cortical neurons and their adjacent axons occurs in the acute phase after traumatic brain injury, possibly related to shear forces and diffuse axonal injury (Gennarelli *et al*., 1982).

The third research hypothesis tested in this study was inspired by the observation that high-velocity impact traumatic brain injury is associated with high mortality and morbidity figures (Adekoya and Majumder, 2004; Walilko *et al*., 2005; Langlois *et al*., 2006*b*; Minino *et al*., 2006). There is experimental and human post-mortem evidence that high-velocity impact traumatic brain injury is associated with substantial diffuse axonal injury and loss of cortical neurons (Gennarelli *et al*., 1982; Graham *et al*., 1992, 2005; Hall *et al*., 2005; Deng *et al*., 2007). Due to small patient numbers, the results of the present study need to be interpreted with caution. The microdialysis *in vivo* data support the experimental and post-mortem observations. The highest extracellular fluid NfH levels were found following high-velocity impact traumatic brain injury. This argument is further strengthened by a body of literature describing widespread brain atrophy in traumatic brain injury (reviewed in Levine *et al*., 2006). Longitudinal

volumetric MRI data suggest that ~1.43% of the total brain volume may be lost following traumatic brain injury (Trivedi *et al*., 2007). About 69% of the patients show an increase in ventricular volume within 2 months of mild to moderate traumatic brain injury (Poca *et al*., 2005). Moreover *N*-acetylaspartate, another biomarker for neuronal loss, was found to decrease by ~12% in a traumatic brain injury cohort who suffered ~1.09% of total brain atrophy over one year (Cohen *et al*., 2007). An important limitation not taken into account by our or any of the cited studies is that the velocity of road traffic accidents varies and falls happen from different heights. Therefore combining patients with road traffic accidents and assault into one category (high-velocity injury) is subject to criticism. Additional statistical analyses splitting the patients into three different groups: road traffic accidents, assault and fall were in line with the results of dichotomized groups. Again, numbers for these analyses were even smaller, further decreasing the power of the study. A possible approach for future studies, to analyse the strength of impact more accurately, could be to calculate the *g*–force (m/s) at impact from an individual patient's weight, the estimated road traffic accident velocity and height of fall. There is increasing concern for high-velocity injuries causing diffuse axonal injury in sport activities (Gieron *et al*., 1998; Walilko *et al*., 2005), in road traffic accidents (Kirkpatrick, 1983; Corbo and Tripathi, 2004) and armed conflict (Suneson *et al*., 1990; Bakir *et al*., 2005). The observation that diffuse axonal injury may occur following high pressure waves (Suneson *et al*., 1990) is interesting and could be further tested using extracellular fluid NfH as a biomarker.

The fourth hypothesis tested was that extracellular fluid NfH levels were related to the type of injury seen on CT brain imaging, as suggested by the IMPACT studies (Steyerberg *et al*., 2008). Higher extracellular fluid NfH levels were found in the presence of traumatic subarachnoid blood, but a confounding factor may be that all of these patients died. The present study was underpowered to allow for a multivariate analysis to exclude a possible bias as recommended (Lingsma *et al*., 2010). For the same reason, one would need to be careful to extrapolate from the absence of such significance based on either the Marshall classification (Marshall *et al*., 1992) or the presence or an extradural haematoma (Steyerberg *et al*., 2008) from our data. Additionally the choice to place the microdialysis catheter in the pericontusional tissue meant that it was remote from the extradural haematoma in all patients (see Patient 1, 8 and 9 in Fig. 5). Future studies investigating a possible effect of extradural haematoma on the adjacent brain tissue may be more informative if the microdialysis catheter were placed adjacent to the extradural haematoma. For the present study, diffuse axonal injury due to high-velocity injury seems a more logical explanation for elevated extracellular fluid NfH levels.

The fifth hypothesis tested was whether extracellular fluid NfH levels were correlated with physiological parameters that are related to injury severity and outcome in traumatic brain injury. For didactic reasons, the four parameters investigated are summarized in Fig. 7C, E, G and I, adjacent to the raw data.

(i) Strong correlations were found between extracellular fluid NfH levels and the extracellular fluid lactate to pyruvate ratio. The data are consistent with observations suggesting that an anaerobic metabolism/ischaemia causes an increase in the lactate to pyruvate ratio (Enblad *et al*., 2001; Hutchinson *et al*., 2002; Belli *et al*., 2008), and relates to neuronal loss (Fig. 7C). However, it is still uncertain whether this is an inexorable pathological cascade, as others have found that a metabolic crisis can also occur without evidence for ischaemic tissue damage (Vespa *et al*., 2005). We propose that extracellular fluid NfH levels provide a sensitive tool for investigating under which circumstances a high lactate to pyruvate ratio may be related to neuronal loss (Fig. 7C).

(ii) Correlations were found between extracellular fluid NfH levels and the systemic blood pressure. It is well established that arterial blood pressure resuscitation is important to improve outcome after traumatic brain injury (Butcher *et al*., 2007; Stiver and Manley, 2008). Our findings raise the question as to whether early and rigorous arterial blood pressure resuscitation could reduce neuronal loss in traumatic brain injury. Extracellular fluid NfH levels could be used as a secondary outcome measure to test this hypothesis (Fig. 7E).

(iii) Moderately strong correlations were found between extracellular fluid NfH levels and brain tissue oxygen levels. This finding is in line with established experimental models showing that oxygen toxicity results in neuronal loss (Arieli *et al*., 2008). Experience in humans is possibly biased because most data on oxygen toxicity come from prolonged hyperbaric conditions during diving (Arieli *et al*., 2006). New data suggest that short periods (1–2 h) of normobaric hyperoxia may improve the aerobic metabolism and cerebral blood flow (Shin *et al*., 2007; Nortje *et al*., 2008; Tisdall *et al*., 2008). Additionally, there is considerable heterogeneity for cerebral blood flow and oxygen utilization between patients (Coles *et al*., 2009). At present the routine clinical use of prolonged hyperoxia is not recommended (Diringer, 2008), but extracellular fluid NfH levels offer a potential safety biomarker for future trials investigating whether targeted short normobaric hyperoxia may emerge as a neuroprotective treatment strategy (Fig. 7G).

(iv) Finally extracellular fluid NfH levels were related to the brain temperature. Importantly, all correlations of brain temperature with extracellular fluid NfH occurred in the acute phase during which rapid hypothermia might have its strongest neuroprotective mechanism (McIntyre *et al*., 2003; Polderman, 2008; Bayir *et al*., 2009; Ma *et al*., 2009). Extracellular fluid NfH levels should be used as an exclusion criteria and secondary outcome measure for future trials of hypothermia in traumatic brain injury (Fig. 7I).

The sixth and the last hypothesis tested in this study was whether extracellular fluid NfH levels are of prognostic value after traumatic brain injury. We note that the mortality in our study is higher than expected from other studies (Steyerberg *et al*., 2008). This may in part be explained by the fact that initial patient recruitment also included patients with traumatic brain injury with milder injury ($n = 5$), but unfortunately a 20 kDa

microdialysis catheter was inserted and the collected extracellular fluid was, therefore, not suitable for the clinical part of this study. In this small study, the profile of extracellular fluid NfH levels in the initial 12 h following traumatic brain injury predicted mortality with an odds ratio of 7.68. The odds ratio for extracellular fluid NfH levels compared favourably to the Glasgow Coma Score (GCS, odds ratio 4.13) and other clinical predictors derived from the large IMPACT data set on 8509 patients with traumatic brain injury (motor score of the GCS 1.0–5.7) (Steyerberg *et al*., 2008).

In conclusion, this translational proof of principle study describes a novel neuronal proteolytic pathway responsible for the release of a specific protein biomarker into the human extracellular fluid. Quantification of this biomarker—extracellular fluid NfH—seems feasible, allowing for *in vivo* monitoring of neurodegeneration in traumatic brain injury. The limited number of cases in this study prevents generalization from our data. The *in vivo* data support experimental, post-mortem and imaging data, suggesting that neuronal loss is likely to be most extensive following high-velocity impact traumatic brain injury. The data also suggest that extracellular fluid NfH levels may be a useful biomarker in this context and might predict poor functional outcome.

Funding

Wellcome Clinical Research Fellow (Grant No. 075608 to M.T.); Department of Health's National Institute for Health Research Centres funding scheme, University College London Hospitals (partial). This work was undertaken at UCLH/UCL, who received a proportion of funding from the Department of Health's NIHR Biomedical Research Centre funding scheme.

Conflict of interest: Axel Petzold is named as inventor of a patent filed on the discovery of the biomarkers in this study and may in the future benefit from royalties.

Supplementary material

Supplementary material is available at *Brain* online.

References

Adekoya N, Majumder R. Fatal traumatic brain injury, West Virginia, 1989–1998. Public Health Rep 2004; 119: 486–92.

Afinowi R, Keir G, Smith M, Kitchen N, Petzold A. Improving the Recovery of S100B Protein in Cerebral Microdialysis: implications for Multimodal Monitoring in Neurocritical Care. Neuroscience Methods 2009; 181: 95–9.

Arieli R, Arieli Y, Daskalovic Y, Eynan M, Abramovich A. CNS oxygen toxicity in closed-circuit diving: signs and symptoms before loss of consciousness. Aviat Space Environ Med 2006; 77: 1153–7.

Arieli R, Truman M, Abramovich A. Recovery from central nervous system oxygen toxicity in the rat at oxygen pressures between 100 and 300 kPa. Eur J Appl Physiol 2008; 104: 867–71.

Bakir A, Temiz C, Umur S, Aydin V, Torun F. High-velocity gunshot wounds to the head: analysis of 135 patients. Neurol Med Chir 2005; 45: 281–7.

Bayir H, Adelson PD, Wisniewski SR, Shore P, Lai Y, Brown D, et al. Therapeutic hypothermia preserves antioxidant defenses after severe traumatic brain injury in infants and children. Crit Care Med 2009; 37: 689–95.

Bellander BM, Cantais E, Enblad P, Hutchinson P, Nordstrom CH, Robertson C, et al. Consensus meeting on microdialysis in neurointensive care. Intensive Care Med 2004; 30: 2166–9.

Belli A, Sen J, Petzold A, Russo S, Kitchen N, Smith M. Metabolic failure precedes intracranial pressure rises in traumatic brain injury: a microdialysis study. Acta Neurochir 2008; 150: 461–9.

Blaber SI, Scarisbrick IA, Bernett MJ, Dhanarajan P, Seavy MA, Jin Y, et al. Enzymatic properties of rat myelencephalon-specific protease. Biochemistry 2002; 41: 1165–73.

Boulware KT, Daugherty PS. Protease specificity determination by using cellular libraries of peptide substrates (CLiPS). Proc Natl Acad Sci USA 2006; 103: 7583–8.

Buki A, Povlishock JT. All roads lead to disconnection? -Traumatic axonal injury revisited. Acta Neurochir 2006; 148: 181–93.

Butcher I, Maas AI, Lu J, Marmarou A, Murray GD, Mushkudiani NA, et al. Prognostic value of admission blood pressure in traumatic brain injury: results from the IMPACT study. J Neurotrauma 2007; 24: 294–302.

Cohen BA, Inglese M, Rusinek H, Babb JS, Grossman RI, Gonen O. Proton MR spectroscopy and MRI-volumetry in mild traumatic brain injury. AJNR Am J Neuroradiol 2007; 28: 907–13.

Coles J, Cunningham A, Salvador R, Chatfield D, Carpenter A, Pickard J, et al. Early metabolic characteristics of lesion and nonlesion tissue after head injury. J Cereb Blood Flow Metab 2009; 29: 965–75.

Corbo J, Tripathi P. Delayed presentation of diffuse axonal injury: a case report. Ann Emerg Med 2004; 44: 57–60.

Dashiell SM, Tanner SL, Pant HC, Quarles RH. Myelin-associated glycoprotein modulates expression and phosphorylation of neuronal cytoskeletal elements and their associated kinases. J Neurochem 2002; 81: 1263–72.

Deng Y, Thompson BM, Gao X, Hall ED. Temporal relationship of peroxynitrite-induced oxidative damage, calpain-mediated cytoskeletal degradation and neurodegeneration after traumatic brain injury. Exp Neurol 2007; 205: 154–65.

Dikmen SS, Ross BL, Machamer JE, Temkin NR. One year psychosocial outcome in head injury. J Int Neuropsychol Soc 1995; 1: 67–77.

Diringer MN. Hyperoxia: good or bad for the injured brain? Curr Opin Crit Care 2008; 14: 167–71.

Drubin DG, Feinstein SC, Shooter EM, Kirschner MW. Nerve growth factor-induced neurite outgrowth in pc12 cells involves the coordinate induction of microtubule assembly and assembly-promoting factors. J Cell Biol 1985; 101 (5 Pt 1): 1799–807.

Enblad P, Frykholm P, Valtysson J, Silander HC, Andersson J, Fasth KJ, et al. Middle cerebral artery occlusion and reperfusion in primates monitored by microdialysis and sequential positron emission tomography. Stroke 2001; 32: 1574–80.

Ericsson C, Peredo I, Nister M. Optimized protein extraction from cryopreserved brain tissue samples. Acta Oncol 2007; 46: 10–20.

Gennarelli T, Thibault L, Adams J, Graham DI, Thompson CJ, Marcincin RP. Diffuse axonal injury and traumatic coma in the primate. Ann Neurol 1982; 12: 564–74.

Gieron MA, Korthals JK, Riggs CD. Diffuse axonal injury without direct head trauma and with delayed onset of coma. Pediatr Neurol 1998; 19: 382–4.

Graham DI, Clark JC, Adams JH, Gennarelli TA. Diffuse axonal injury caused by assault. J Clin Pathol 1992; 45: 840–1.

Graham DI, Maxwell WL, Adams JH, Jennett B. Novel aspects of the neuropathology of the vegetative state after blunt head injury. Prog Brain Res 2005; 150: 445–55.

Greenwood J, Troncoso J, Costello A, Johnson G. Phosphorylation modulates calpain-mediated proteolysis and calmodulin binding of the 200-kDa and 160-kDa neurofilament proteins. J Neurochem 1993; 61: 191–99.

Hall ED, Sullivan PG, Gibson TR, Pavel KM, Thompson BM, Scheff SW. Spatial and temporal characteristics of neurodegeneration after

controlled cortical impact in mice: more than a focal brain injury. J Neurotrauma 2005; 22: 252–65.
Hutchinson PJ, Gupta AK, Fryer TF, Al-Rawi PG, Chatfield DA, Coles JP, et al. Correlation between cerebral blood flow, substrate delivery, and metabolism in head injury: a combined microdialysis and triple oxygen positron emission tomography study. J Cereb Blood Flow Metab 2002; 22: 735–45.
Hutchinson PJ, O'Connell MT, Nortje J, Smith P, Al-Rawi PG, Gupta AK, et al. Cerebral microdialysis methodology–evaluation of 20 kDa and 100 kDa catheters. Physiol Meas 2005; 26: 423–8.
Kirkpatrick JB. Head-in-motion contusions in young adults. Acta Neurochir Suppl 1983; 32: 115–7.
Kitson R, Desai S. Us guidance on traumatic brain injury management. Critical Care 2005; 9: E28.
Langlois JA, Rutland-Brown W, Thomas KE. Traumatic Brain Injury in the United States: Emergency Department Visits, Hospitalizations, and Deaths. Centers for Disease Control and Prevention, National Center for Injury Prevention and Control 2006a: 1–56.
Langlois JA, Rutland-Brown W, Wald MM. The epidemiology and impact of traumatic brain injury: a brief overview. J Head Trauma Rehabil 2006b; 21: 375–8.
Lee VM. Neurofilament protein abnormalities in PC12 cells: comparison with neurofilament proteins of normal cultured rat sympathetic neurons. J Neurosci 1985; 5: 3039–46.
Leissring MA. The AbetaCs of Abeta-cleaving proteases. J Biol Chem 2008; 283: 29645–9.
Levine B, Fujiwara E, O'Connor C, Richard N, Kovacevic N, Mandic M, et al. In vivo characterization of traumatic brain injury neuropathology with structural and functional neuroimaging. J Neurotrauma 2006; 23: 1396–411.
Light A, Janska H. Enterokinase (enteropeptidase): comparative aspects. Trends Biochem Sci 1989; 14: 110–2.
Lindenbaum MH, Carbonetto S, Mushynski WE. Nerve growth factor enhances the synthesis, phosphorylation, and metabolic stability of neurofilament proteins in pc12 cells. J Biol Chem 1987; 262: 605–10.
Lingsma HF, Roozenbeek B, Steyerberg EW, Murray GD, Maas AIR. Early prognosis in traumatic brain injury: from prophecies to predictions. Lancet Neurol 2010; 9: 543–54.
Littell R, Henry P, Ammerman C. Statistical analysis of repeated measured data using SAS procedures. J Anim Sci 1998; 76: 1216–31.
Ma M, Matthews BT, Lampe JW, Meaney DF, Shofer FS, Neumar RW. Immediate short-duration hypothermia provides long-term protection in an in vivo model of traumatic axonal injury. Exp Neurol 2009; 215: 119–27.
Marshall L, Marshall S, Klauber M, van Berkum C, Eisenberg H, Jane JA, et al. The diagnosis of head injury requires a classification based on computed axial tomography. J Neurotrauma 1992; 9: S287–92.
McGinn MJ, Kelley BJ, Akinyi L, Oli MW, Liu MC, Hayes RL, et al. Biochemical, structural, and biomarker evidence for calpain-mediated cytoskeletal change after diffuse brain injury uncomplicated by contusion. J Neuropathol Exp Neurol 2009; 68: 241–9.
McIntyre LA, Fergusson DA, Hebert PC, Moher D, Hutchison JS. Prolonged therapeutic hypothermia after traumatic brain injury in adults: a systematic review. JAMA 2003; 289: 2992–9.
Minino AM, Anderson RN, Fingerhut LA, Boudreault MA, Warner M. Deaths: injuries, 2002. Natl Vital Stat Rep 2006; 54: 1–124.
Nixon R, Sihag R. Neurofilament phosphorylation: a new look at regulation and function. Trends Neurosci 1991; 14: 501–6.
Nortje J, Coles JP, Timofeev I, Fryer TD, Aigbirhio FI, Smielewski P, et al. Effect of hyperoxia on regional oxygenation and metabolism after severe traumatic brain injury: preliminary findings. Crit Care Med 2008; 36: 273–81.
Pavlov I. The work of the digestive glands, 2nd edn. Thompson WH, trans.London, UK: Ballantyne; 1910.
Petzold A. Neurofilament phosphoforms: surrogate markers for axonal injury, degeneration & loss. J Neurol Sci 2005; 233: 183–98.
Petzold A. CSF biomarkers for improved prognostic accuracy in acute CNS disease. Neurological Research 2007; 29: 691–708.
Petzold A, Gveric D, Groves M, Schmierer K, Grant D, Chapman M, et al. Phosphorylation and compactness of neurofilaments in multiple sclerosis: indicators of axonal pathology. Exp Neurol 2008; 213: 326–35.
Petzold A, Keir G, Green A, Giovannoni G, Thompson E. A specific ELISA for measuring neurofilament heavy chain phosphoforms. J Immunol Methods 2003; 278: 179–90.
Petzold A, Shaw G. Comparison of two ELISA methods for measuring levels of the phosphorylated neurofilament heavy chain. J Immunol Methods 2007; 319: 34–40.
Pittman RN, Wang S, DiBenedetto AJ, Mills JC. A system for characterizing cellular and molecular events in programmed neuronal cell death. J Neurosci 1993; 13: 3669–80.
Poca MA, Sahuquillo J, Mataro M, Benejam B, Arikan F, Baguena M. Ventricular enlargement after moderate or severe head injury: a frequent and neglected problem. J Neurotrauma 2005; 22: 1303–10.
Polderman KH. Induced hypothermia and fever control for prevention and treatment of neurological injuries. Lancet 2008; 371: 1955–69.
Posmantur R, Hayes RL, Dixon CE, Taft WC. Neurofilament 68 and neurofilament 200 protein levels decrease after traumatic brain injury. J Neurotrauma 1994; 11: 533–45.
Posmantur RM, Zhao X, Kampfl A, Clifton GL, Hayes RL. Immunoblot analyses of the relative contributions of cysteine and aspartic proteases to neurofilament breakdown products following experimental brain injury in rats. Neurochem Res 1998; 23: 1265–76.
Povlishock J. Traumatically induced axonal injury: pathogenesis and pathobiological implications. Brain Pathol 1992; 2: 1–12.
Sairanen T, Szepesi R, Karjalainen-Lindsberg M-L, Saksi J, Paetau A, Lindsberg PJ. Neuronal caspase-3 and parp-1 correlate differentially with apoptosis and necrosis in ischemic human stroke. Acta Neuropathol 2009; 118: 541–52.
Schepowalnikow N. Dissertation St. Petersburg. PhD thesis; 1899.
Schutze K, Niyaz Y, Stich M, Buchstaller A. Noncontact laser microdissection and catapulting for pure sample capture. Methods Cell Biol 2007; 82: 649–73.
Shaw G. Neurofilaments. New York: Springer-Verlag; 1998.
Shin HK, Dunn AK, Jones PB, Boas DA, Lo EH, Moskowitz MA, et al. Normobaric hyperoxia improves cerebral blood flow and oxygenation, and inhibits peri-infarct depolarizations in experimental focal ischaemia. Brain 2007; 130: 1631–42.
Smith M. Diffuse axonal injury in adults. Trauma 2003; 5: 1–8.
Steyerberg EW, Mushkudiani N, Perel P, Butcher I, Lu J, McHugh GS, et al. Predicting outcome after traumatic brain injury: development and international validation of prognostic scores based on admission characteristics. PLoS Med 2008; 5: e165, discussion e165.
Stiver SI, Manley GT. Prehospital management of traumatic brain injury. Neurosurg Focus 2008; 25: E5.
Sulejczak D, Grieb P, Walski M, Frontczak-Baniewicz M. Apoptotic death of cortical neurons following surgical brain injury. Folia Neuropathol 2008; 46: 213–9.
Suneson A, Hansson HA, Seeman T. Pressure wave injuries to the nervous system caused by high-energy missile extremity impact: Part II. distant effects on the central nervous system-a light and electron microscopic study on pigs. J Trauma 1990; 30: 295–306.
Teasdale G, Pettigrew L, Wilson J, Murray G, Jennett B. Analyzing outcome of treatment of severe head injury: a review and update on advancing the use of the Glasgow Outcome Scale. J Neurotrauma 1998; 15: 587–97.
Tisdall M, Smith M. Cerebral microdialysis: research technique or clinical tool. Br J Anaesth 2006; 97: 18–25.
Tisdall MM, Tachtsidis I, Leung TS, Elwell CE, Smith M. Increase in cerebral aerobic metabolism by normobaric hyperoxia after traumatic brain injury. J Neurosurg 2008; 109: 424–32.
Trivedi MA, Ward MA, Hess TM, Gale SD, Dempsey RJ, Rowley HA, et al. Longitudinal changes in global brain volume between 79 and 409 days after traumatic brain injury: relationship with duration of coma. J Neurotrauma 2007; 24: 766–71.

Umschwief G, Shein NA, Alexandrovich AG, Trembovler V, Horowitz M, Shohami E. Heat acclimation provides sustained improvement in functional recovery and attenuates apoptosis after traumatic brain injury. J Cereb Blood Flow Metab 2010; 30: 616–27.

Vespa P, Bergsneider M, Hattori N, Wu HM, Huang SC, Martin NA, et al. Metabolic crisis without brain ischemia is common after traumatic brain injury: a combined microdialysis and positron emission tomography study. J Cereb Blood Flow Metab 2005; 25: 763–74.

Vilen ST, Nyberg P, Hukkanen M, Sutinen M, Ylipalosaari M, Bjartell A, et al. Intracellular co-localization of trypsin-2 and matrix metalloprotease-9: possible proteolytic cascade of trypsin-2, MMP-9 and enterokinase in carcinoma. Exp Cell Res 2008; 314: 914–26.

Walilko TJ, Viano DC, Bir CA. Biomechanics of the head for Olympic boxer punches to the face. Br J Sports Med 2005; 39: 710–9.

Wiegand U, Corbach S, Minn A, Kang J, Muller-Hill B. Cloning of the cDNA encoding human brain trypsinogen and characterization of its product. Gene 1993; 136: 167–75.

Zhang J, Yoganandan N, Pintar FA, Gennarelli TA. Brain strains in vehicle impact tests. Annu Proc Assoc Adv Automot Med 2006; 50: 1–12.